

Supporting Information for

**Effect of spin-orbit coupling on phonon-mediated magnetic relaxation in a series of zero-valent vanadium, niobium, and tantalum isocyanide complexes**

Khetpakorn Chakarawet,<sup>a</sup> Mihail Atanasov,<sup>bc</sup> John E. Ellis,<sup>d</sup> Wayne W. Lukens Jr.,<sup>e</sup> Victor G. Young Jr.,<sup>d</sup> Ruchira Chatterjee,<sup>f</sup> Frank Neese<sup>b</sup> and Jeffrey R. Long<sup>\*agh</sup>

<sup>a</sup>Department of Chemistry and <sup>g</sup>Department of Chemical and Biomolecular Engineering, University of California Berkeley, Berkeley, California 94720, United States

<sup>b</sup>Max-Planck Institut für Kohlenforschung, Kaiser-Wilhelm-Platz 1, D-45470 Mülheim an der Ruhr, Germany

<sup>c</sup>Institute of General and Inorganic Chemistry, Bulgarian Academy of Science, Akad. G. Bontchev Street, Bl.11, 1113 Sofia, Bulgaria

<sup>d</sup>Department of Chemistry, University of Minnesota, Minneapolis, Minnesota 55455, United States

<sup>e</sup>Chemical Sciences Division, Lawrence Berkeley National Laboratory, Berkeley, California 94720, United States

<sup>f</sup>Molecular Biophysics and Integrated Bioimaging Division, Lawrence Berkeley National Laboratory, Berkeley, California 94720, United States

<sup>h</sup>Materials Sciences Division, Lawrence Berkeley National Laboratory, Berkeley, California 94720, United States

<b>Table of Contents</b>	<b>page</b>
Experimental Details	S2
X-ray Crystallography	S6
Electrochemistry	S9
Electron Paramagnetic Resonance Spectroscopy	S11
Magnetic Measurements	S15
Relaxation Dynamics	S25
Density Functional Theory Calculations	S28
Correlated Electronic Calculations	S29
Geometry Optimized Coordinates	S38
References	S56

**General comments on the synthesis of 1.** All operations were carried out under a dry, dioxygen-free atmosphere of argon gas using Schlenk-line and glove box techniques. Literature procedures were employed to prepare  $\text{VCl}_3(\text{THF})_3$  (THF = tetrahydrofuran),<sup>1</sup> and  $\text{CNDipp}$  (Dipp = 2,6-diisopropylphenyl).<sup>2</sup> Other reagents and solvents were obtained from commercial sources and freed of dioxygen and moisture by standard methods prior to use. The synthesis of (**1**) was similar to that of Barybin's related  $\text{V}(\text{CNXyl})_6$ , Xyl = 2,6-dimethylphenyl,<sup>3</sup> except the labile  $\text{V}(0)$  precursor,  $\text{V}(\text{MeC}_{10}\text{H}_7)_2$  ( $\text{MeC}_{10}\text{H}_7$  = 1-methylnaphthalene) was prepared *in situ* by oxidation of the anionic precursor with  $\text{MoO}_3$ , rather than alumina, and reacted directly with  $\text{CNDipp}$ . Because prior isolated yields of  $\text{V}(\text{MeC}_{10}\text{H}_7)_2$  never exceeded 45%,<sup>3</sup> and  $\text{CNDipp}$  is a valuable material, the following synthesis of **1** employed slightly less than a 3:1 mole ratio of  $\text{CNDipp}$  to  $\text{VCl}_3(\text{THF})_3$ . Satisfactorily pure **1** was isolated in 72% yield by this facile method. Microanalysis of **1** was obtained at the CENTC Elemental Analysis Facility by Dr. William W. Brennessel of the University of Rochester, Rochester, New York, USA.

**Preparation of  $\text{V}(\text{CNDipp})_6$  (**1**).** A deep green solution of  $\text{Na}[\text{MeC}_{10}\text{H}_7]$  was obtained by adding 1-methylnaphthalene (3.50 mL; 3.50 g, 24.6 mmol) in THF (50 mL) to a 500 mL flask containing sodium metal (0.374 g, 16.3 mmol) cut into 10 small pieces and THF (50 mL). The mixture was rapidly stirred (~500 rpm) with a glass-covered magnetic stir bar for 5 h at 293 K, in the dark to minimize photo-oxidation of the 1-methylnaphthalene radical anion. The mixture was then cooled to 200 K and a cold (200 K) solution/slurry of  $\text{VCl}_3(\text{THF})_3$  (1.500 g, 4.015 mmol) in THF (100 mL) was transferred by cannula to the cold solution of  $\text{Na}[\text{MeC}_{10}\text{H}_7]$ . With constant stirring, the reaction mixture was slowly warmed, while immersed in a Dewar, over a period of 20 h to 293 K. Powdered  $\text{MoO}_3$  (0.867 g, 4.21 mmol) was then added all at once to the stirred reaction mixture at 293 K, whereupon over a period of 2 h, the color changed from a deep red-brown to a dark red-maroon hue, characteristic of  $\text{V}(\text{MeC}_{10}\text{H}_7)_2$ . Neat  $\text{CNDipp}$  (2.20 g, 11.7 mmol) was subsequently added to the reaction mixture via syringe, with stirring, and within minutes the mixture changed to a deep plum color. Following an additional stirring for 24 h at 293 K, the quite turbid reaction mixture was filtered through a 5 cm column of diatomaceous earth (filter-aid) in a medium porosity or P3 glass frit to afford an intense purple solution, quite similar to the color of aqueous potassium permanganate. Removal of solvent *in vacuo* afforded an oily semi-solid, which was taken up in toluene (100 mL) and filtered, as before. Subsequent removal of solvent, followed by trituration with heptane (50 mL), to remove 1-methylnaphthalene, which can be isolated and re-used, resulted in the deposition of microcrystalline product. This solid was separated by filtration, washed twice with 10 mL portions of heptane (in which the product is only very slightly soluble), and dried at 293 K *in vacuo*. Free-flowing, golden-brown, microcrystalline and highly air-sensitive **1** of satisfactory purity was thereby obtained (1.634 g, 72% yield, based on use of 2.9 equiv. of  $\text{CNDipp}$ ). X-ray quality crystals of **1** were grown from THF/pentane at 263 K. Anal. Calcd for  $\text{C}_{78}\text{H}_{102}\text{N}_6\text{V}$ : C, 79.76; H, 8.75; N, 7.16%. Found: C, 78.93; H, 8.70; N, 6.95. IR ( $\nu$  (CN), toluene) 1946 (vs, br)  $\text{cm}^{-1}$ .  $^1\text{H}$  NMR (500 MHz, 293 K, toluene- $d_8$ ):  $\delta$  -2.66 (t, 1 H, *p*-H), 1.20 (d, 12 H,  $(\text{CH}_3)_2\text{CH}$ ), 7.61 (m, 2 H,  $(\text{CH}_3)_2\text{CH}$ ), 14.23 (d, 2 H, *m*-H) ppm.  $^{13}\text{C}\{^1\text{H}\}$  NMR (125 MHz, 293 K, toluene- $d_8$ ):  $\delta$  -100.7 (*ipso*-C), 8.5 ( $(\text{CH}_3)_2\text{CH}$ ), 39.0 ( $(\text{CH}_3)_2\text{CH}$ ), 93.1 (*m*-C), 182.5 (*p*-C), 341.9 (*o*-C)

ppm. We thank Zachary W. Davis-Gilbert for acquisition of the NMR spectra shown in Figures S2 and S3.

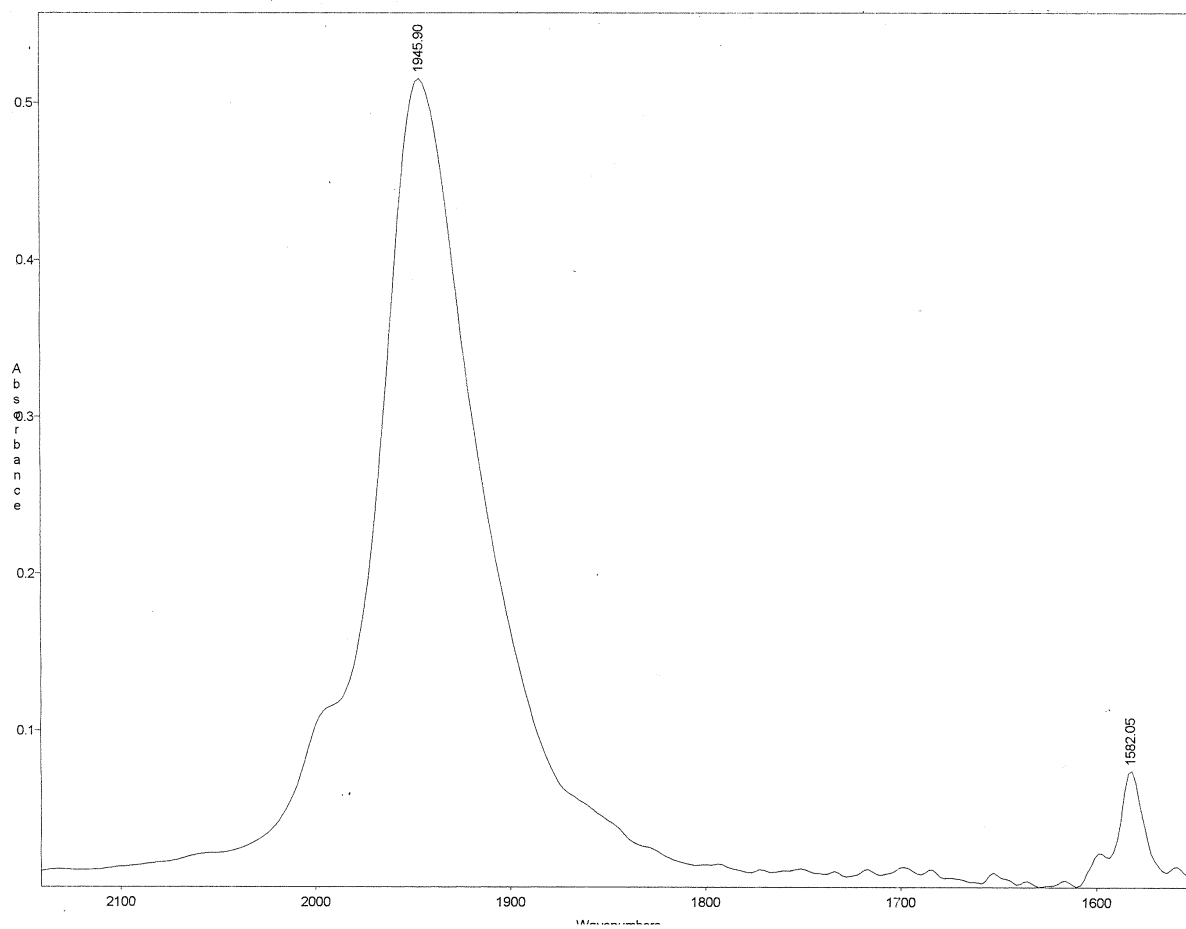


**Figure S1.** IR spectrum of  $V(CNDipp)_6$  (**1**) in toluene ( $\nu(CN) = 1946\text{ cm}^{-1}$ ). The weak peak at  $1582\text{ cm}^{-1}$  is due to the N–C(Dipp) absorption.

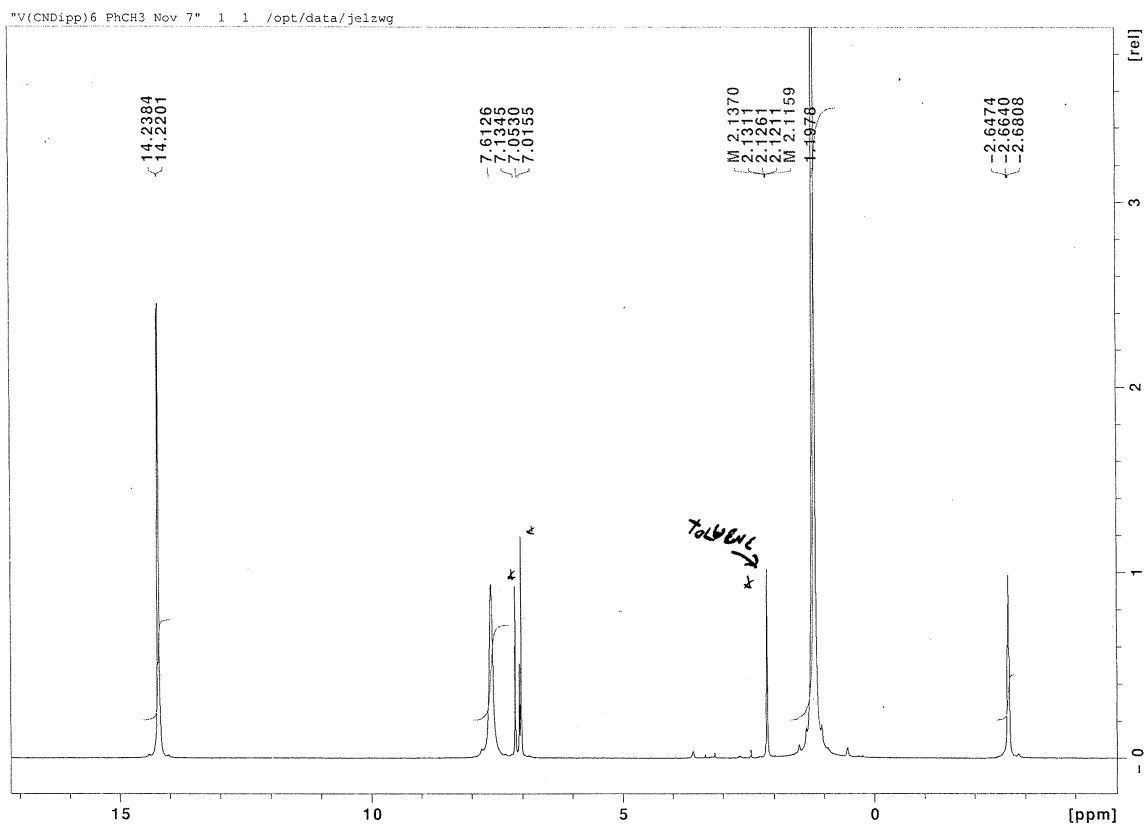


**Figure S2.**  $^1\text{H}$  NMR spectrum of **1** in toluene- $d_8$  at 293 K. Resonances at 7.05, 7.01, and 2.13 ppm marked with asterisks are due to toluene- $d_8$ .

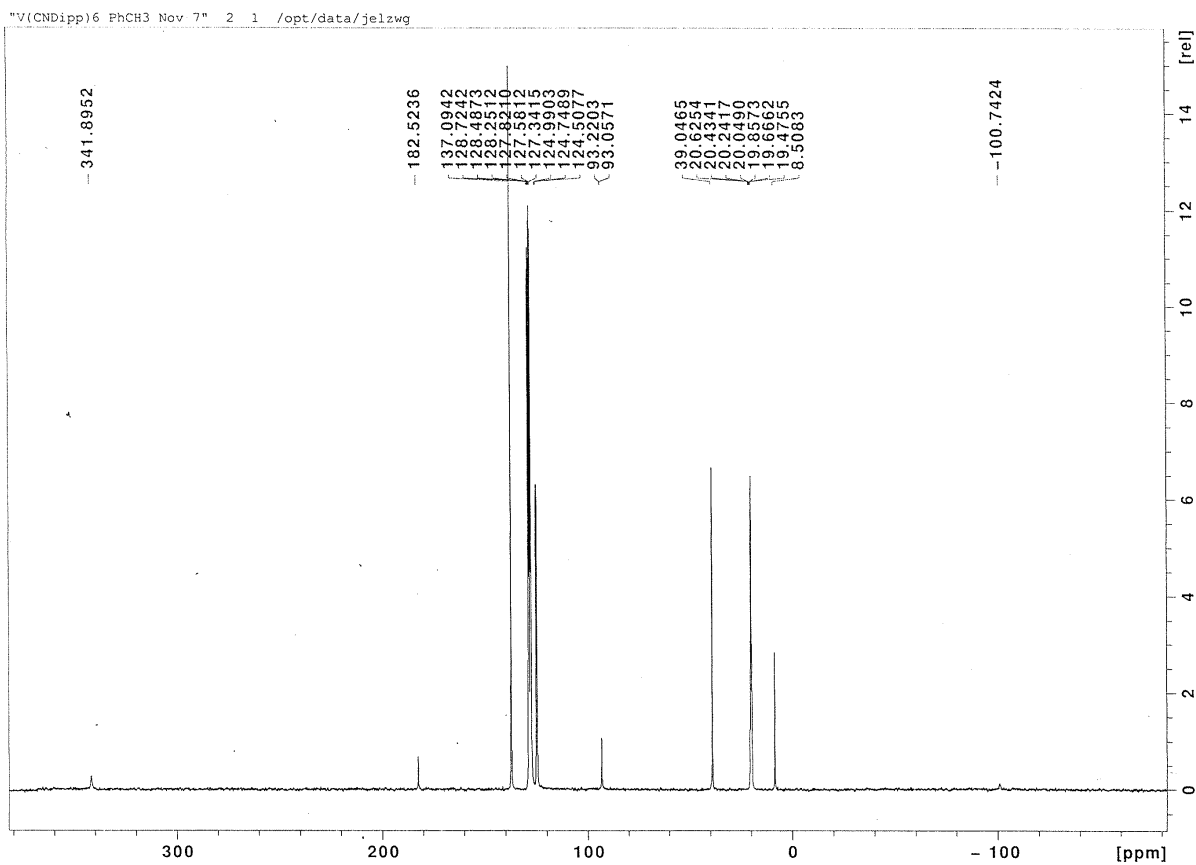


**Figure S3.**  $^{13}\text{C}\{^1\text{H}\}$  NMR spectrum of **1** in toluene- $d_8$  at 293 K. Resonances from 137–124 ppm and multiplet from 20.6–19.5 ppm are due to toluene- $d_8$ .

## X-ray Crystallography

A single crystal of **1** was placed onto the tip of a 0.1 mm diameter glass capillary and mounted on a Bruker APEX-II CCD diffractometer for data collection at 173(2) K. A preliminary set of cell constants was calculated from reflections harvested from three sets of 20 frames. These initial sets of frames were oriented such that orthogonal wedges of reciprocal space were surveyed. The data collection was carried out using Mo- $K\alpha$  radiation (graphite monochromator). A randomly oriented region of reciprocal space was surveyed to the extent of one sphere and to a resolution of 0.77 Å. Four major sections of frames were collected with 0.30° steps in  $\omega$  at four different  $\varphi$  settings and a detector position of  $2\theta = -28^\circ$ . The intensity data were corrected for absorption and decay (SADABS).<sup>4</sup> Final cell constants were calculated from 2953 strong reflections from the actual data collection after integration (SAINT).<sup>5</sup> The structure was solved using SHELXT-2014/5<sup>6</sup> and refined using SHELXL-2014/6.<sup>6</sup> The space group  $R\bar{3}$  was determined based on systematic absences and intensity statistics. A direct-methods solution was calculated that provided most non-hydrogen atoms from the E-map. Full-matrix least squares/difference Fourier cycles were performed which located the remaining non-hydrogen atoms. All non-hydrogen atoms were refined with anisotropic displacement parameters. All hydrogen atoms were placed in ideal positions and refined as riding atoms with relative isotropic displacement parameters. The final full matrix least squares refinement converged to  $R_1 = 0.0499$  and  $wR_2 = 0.1304$  ( $F^2$ , all data).

**Table S1.** Crystal data and structure refinement for V(CNDipp)<sub>6</sub> (**1**)

	V(CNDipp) <sub>6</sub> ( <b>1</b> )
CCDC number	1991804
Empirical formula	VN <sub>6</sub> C <sub>78</sub> H <sub>102</sub>
Formula weight (g/mol)	1174.59
Temperature (K)	173(2)
Wavelength (Å)	0.71073
Crystal system	Trigonal
Space group	<i>R</i> 3
<i>a</i> (Å), $\alpha$ (°)	15.0796(14), 90
<i>b</i> (Å), $\beta$ (°)	15.0796(14), 90
<i>c</i> (Å), $\gamma$ (°)	26.863(3), 120
Volume (Å <sup>3</sup> )	5290.1(11)
<i>Z</i>	3
Density (calculated, g/cm <sup>3</sup> )	1.106
Absorption coefficient (mm <sup>-1</sup> )	0.186
<i>F</i> (000)	1905
Crystal color, morphology	Purple, Rhombohedron
Crystal size (mm <sup>3</sup> )	0.35 × 0.30 × 0.30
$\theta$ range for data collection (°)	1.734 to 27.478
Index ranges	-19 ≤ <i>h</i> ≤ 18 -19 ≤ <i>k</i> ≤ 19 -30 ≤ <i>l</i> ≤ 34
Reflections collected	13448
Independent reflections, <i>R</i> <sub>int</sub>	2691, 0.0366
Completeness to $\theta = 25.242^\circ$	100.0 %
Absorption correction	Semi-empirical from equivalents
Max. and min. transmission	0.5629 and 0.5041
Refinement method	Full-matrix least-squares on <i>F</i> <sup>2</sup>
Data / restraints / parameters	2691 / 345 / 193
Goodness-of-fit on <i>F</i> <sup>2</sup>	1.041
Final <i>R</i> indices [ <i>I</i> > 2σ( <i>I</i> )]	<i>R</i> <sub>1</sub> = 0.0499, <i>wR</i> <sub>2</sub> = 0.1193
<i>R</i> indices (all data)	<i>R</i> <sub>1</sub> = 0.0654, <i>wR</i> <sub>2</sub> = 0.1304
Extinction coefficient	n/a
Largest diff. peak and hole (e <sup>-</sup> ·Å <sup>-3</sup> )	0.307 and -0.326

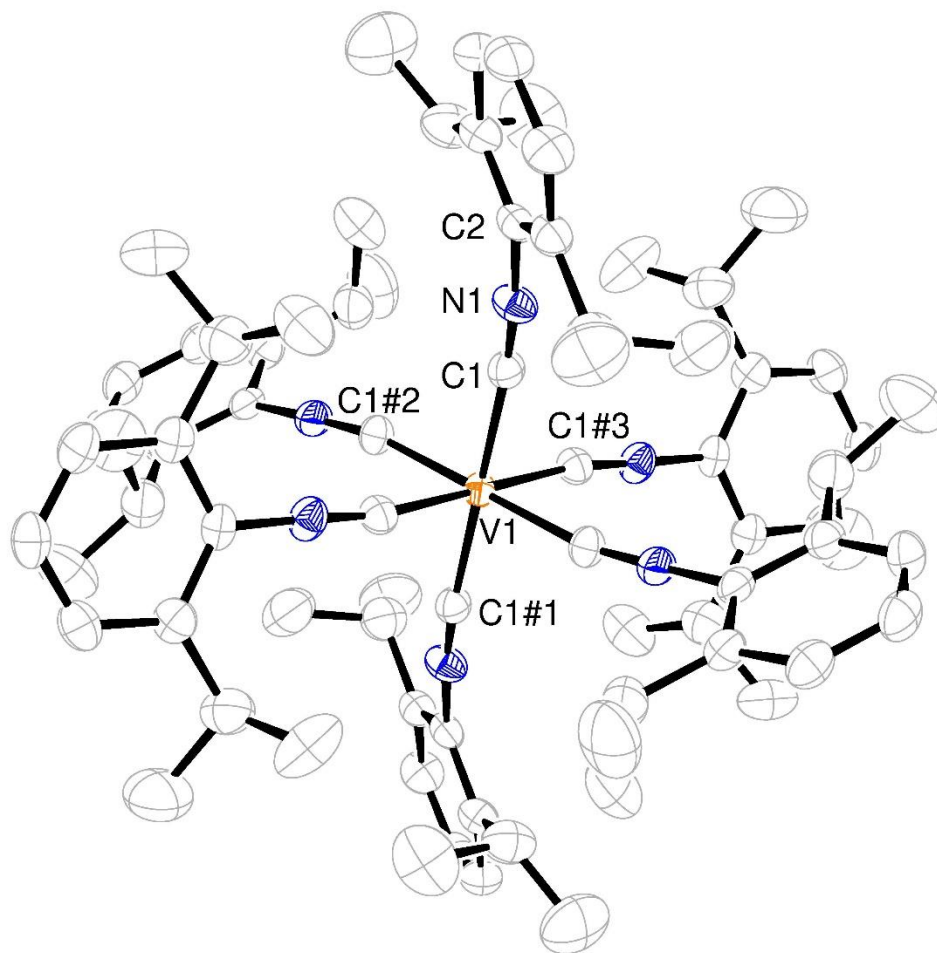


**Figure S4.** Thermal ellipsoids plot of V(CNDipp)<sub>6</sub> (**1**) at the 50% probability level. Disordered components and H atoms are omitted for clarity.

**Table S2.** Selected bond distances (Å) and angles (°) for V(CNDipp)<sub>6</sub> (**1**). The disordered component is marked with the prime (') symbol.

V(1)–C(1)	2.0138(16)	C(1)–V(1)–C(1)#1	180.0
C(1)–N(1)	1.186(3)	C(1)–V(1)–C(1)#2	85.33(6)
N(1)–C(2)	1.389(2)	C(1)–V(1)–C(1)#3	94.67(6)
V(1)–C(1')	2.0138(16)	V(1)–C(1)–N(1)	169.0(4)
C(1')–N(1')	1.188(3)	C(1)–N(1)–C(2)	174.6(8)
N(1')–C(2')	1.391(2)	C(1')–V(1)–C(1')#1	180.0
		C(1')–V(1)–C(1')#2	85.33(6)
		C(1')–V(1)–C(1')#3	94.67(6)
		V(1)–C(1')–N(1')	175.0(5)
		C(1')–N(1')–C(2')	159.0(8)



## Electrochemistry

Cyclic voltammograms of compounds **1–3** and  $V(\text{CNXyl})_6$  (Xyl = 2,6-dimethylphenyl) were recorded using a Bio-Logic SP-200 potentiostat and a three-electrode setup, with Pt working, Pt auxiliary, and Ag wire reference electrodes immersed in a 0.1 M tetra-*n*-butylammonium hexafluorophosphate ( $\text{NBu}_4\text{PF}_6$ ) electrolyte solution in 1,2-difluorobenzene (DFB). The potentials were referenced to the  $[\text{FeCp}_2]^{+/0}$  redox couple, and the voltammograms were recorded at a scan rate of 100 mV/s.

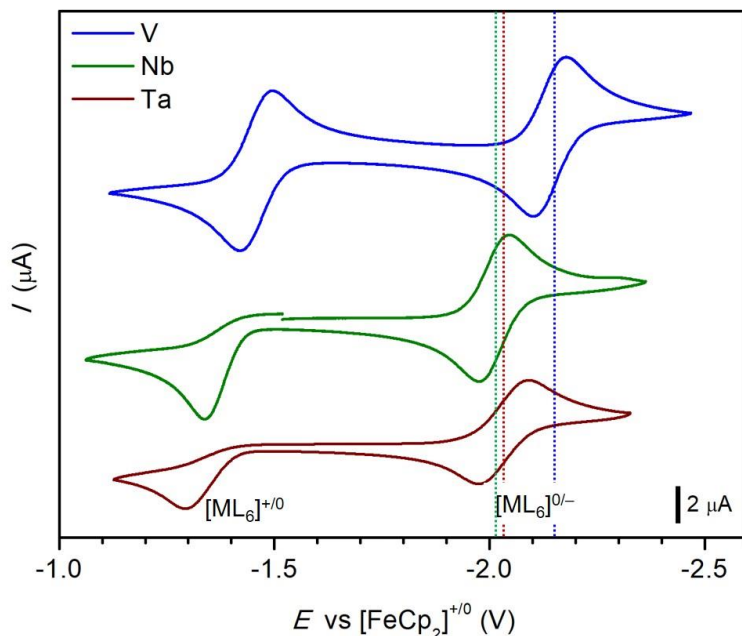


**Figure S5.** Cyclic voltammograms of 1 mM solutions of  $V(\text{CNDipp})_6$  (**1**, blue),  $\text{Nb}(\text{CNDipp})_6$  (**2**, green), and  $\text{Ta}(\text{CNDipp})_6$  (**3**, red) in DFB with 0.1 M  $\text{NBu}_4\text{PF}_6$ . The black rectangle on the lower right of the plot indicates the height of 2  $\mu\text{A}$ . Vertical dotted lines indicate  $E_{1/2}$  potentials.

A reversible one-electron reduction event was observed at  $-2.15$  V (vs.  $[\text{FeCp}_2]^{+/0}$ ) for  $V(\text{CNDipp})_6$ , compared to  $-2.01$  V for  $\text{Nb}(\text{CNDipp})_6$  and  $-2.03$  V for  $\text{Ta}(\text{CNDipp})_6$ . In addition, a reversible one-electron oxidation was observed for  $V(\text{CNDipp})_6$  at  $-1.46$  V, attributable to the formation of  $[\text{V}(\text{CNDipp})_6]^+$  cation. In contrast, oxidation of  $\text{Nb}(\text{CNDipp})_6$  and  $\text{Ta}(\text{CNDipp})_6$  is irreversible, which is hypothesized to be due to the more open coordination sphere of Nb and Ta compared to V in these complexes.

**Table S3.** Potentials (referenced to  $[\text{FeCp}_2]^{+/0}$ ) of the redox events for **1–3**

	$V(\text{CNDipp})_6$ ( <b>1</b> )	$\text{Nb}(\text{CNDipp})_6$ ( <b>2</b> )	$\text{Ta}(\text{CNDipp})_6$ ( <b>3</b> )
$E_{1/2}([\text{ML}_6]^{0/-})$ (V)	$-2.15$	$-2.01$	$-2.03$
$E_{1/2}([\text{VL}_6]^{+/0})$ (V)	$-1.46$	–	–
$E_p([\text{ML}_6]^{+/0})$ (V)	–	$-1.36$	$-1.30$

We also investigated electrochemical behavior of the previously reported zero-valent  $V(CNXyl)_6$  complex.<sup>3</sup> Cyclic voltammograms collected for  $V(CNXyl)_6$  and  $V(CNDipp)_6$  in DFB with 0.1 M  $NBu_4PF_6$  are plotted in Figure S6. Both complexes show three one-electron redox processes, indicating that vanadium oxidation states of +2, +1, 0, and -1 are accessible. Note, however, that the last oxidation of  $V(CNDipp)_6$  (corresponding to formation of  $[V(CNDipp)_6]^{2+}$ ) appears only quasi-reversible; decomposition starts to occur after accessing this doubly oxidized species, warping the shape of other peaks during the scan.

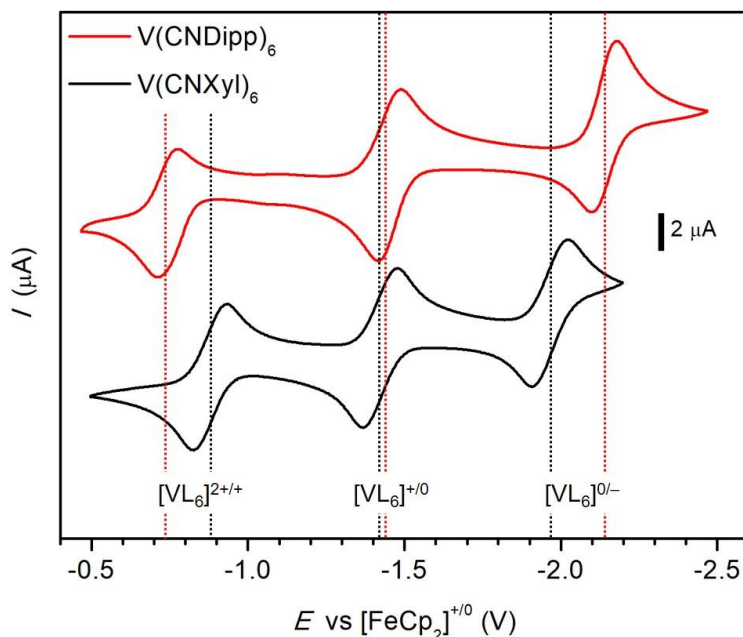


**Figure S6.** Cyclic voltammograms of  $V(CNDipp)_6$  (**1**) (red) and  $V(CNXyl)_6$  (black). The black rectangle on the right indicates the height of 2  $\mu A$ . Vertical dotted lines indicate  $E_{1/2}$  potentials.

**Table S4.** Half-peak potentials (referenced to  $[FeCp_2]^{+/0}$ ) of the redox events for **1** and  $V(CNXyl)_6$ , and calculated comproportionation constants.

	$V(CNDipp)_6$	$V(CNXyl)_6$
$E_{1/2}([VL_6]^{2+/+})$ (V)	-0.75	-0.88
$E_{1/2}([VL_6]^{+/0})$ (V)	-1.46	-1.42
$E_{1/2}([VL_6]^{0/-})$ (V)	-2.15	-1.97
$K_c$ ( $[VL_6]^0$ )	$4.5 \times 10^{11}$	$1.7 \times 10^9$
$K_c$ ( $[VL_6]^+$ )	$1.0 \times 10^{12}$	$1.4 \times 10^9$

## Electron Paramagnetic Resonance Spectroscopy

Crystalline samples of **1–3** were finely powdered and sealed in quartz EPR tubes under argon. Spectra were recorded between 3 and 5 K on a Varian E-12 Century spectrometer equipped with an AIP frequency counter and Varian Gaussmeter previously calibrated using DPPH in the sample cavity. Spectrum of **1** was collected at 5 K using 9.097 GHz microwave irradiation at 50 mW, 3.3 G modulation amplitude. Spectrum of **2** was collected at 5 K using 9.095 GHz microwave irradiation at 50 mW, 0.25 G modulation amplitude. Spectrum of **3** was collected at 3 K using 9.098 GHz microwave irradiation at 50 mW, 1 G modulation amplitude. All spectra were collected with 100 kHz modulation frequency. Simulations were performed using a version of the code ABVG that has been modified to perform least squares fitting using a Pilbrow lineshape.<sup>7,8</sup>

In calculating the  $\eta$  ratio of complexes **1–3**, we adopt a trigonal basis:

$$a_1(t_2): d_{z^2}$$

$$e(t_2): e_x = \sqrt{\frac{2}{3}}d_{xy} - \sqrt{\frac{1}{3}}d_{xz}$$

$$e_y = -\sqrt{\frac{2}{3}}d_{x^2-y^2} - \sqrt{\frac{1}{3}}d_{yz}$$

$$e(e): e_x = \sqrt{\frac{1}{3}}d_{xy} + \sqrt{\frac{2}{3}}d_{xz}$$

$$e_y = \sqrt{\frac{1}{3}}d_{x^2-y^2} + \sqrt{\frac{2}{3}}d_{yz}$$

where the  $z$  Cartesian axis is taken parallel to the  $C_3$  axis, while the  $x$ -axis coincides with one of the three  $C_2$  axes of the  $D_3$  point group. The expressions for the  $g$  tensors in the  ${}^2A_1$  ground states of complexes **1–3** are given in Eqns. (2) and (3) in the main text. In these expressions, the parameter  $\varepsilon = \zeta/\delta_2$  which quantifies the perturbation of the  ${}^2A_1({}^2T_2)$  ground state by the  ${}^2E({}^2E)$  excited states was set to zero; the reason is that  $\delta_2$  has the order of magnitude of the cubic splitting parameter  $10Dq$ , and therefore is much larger than  $\zeta$ . This justifies the omission of  $\varepsilon$  in the expressions (however, this parameter is crucial in tetragonal  $d^9$  systems with an  $d_{x^2-y^2}$  ground state)<sup>9,10</sup>

The solution spectra of **2**, **3**, and  $V(CNXyl)_6$  were collected in a 1 mM toluene solution using a Varian E109 EPR spectrometer equipped with a Model 102 Microwave bridge. Simulations were performed using EasySpin software.<sup>11</sup>

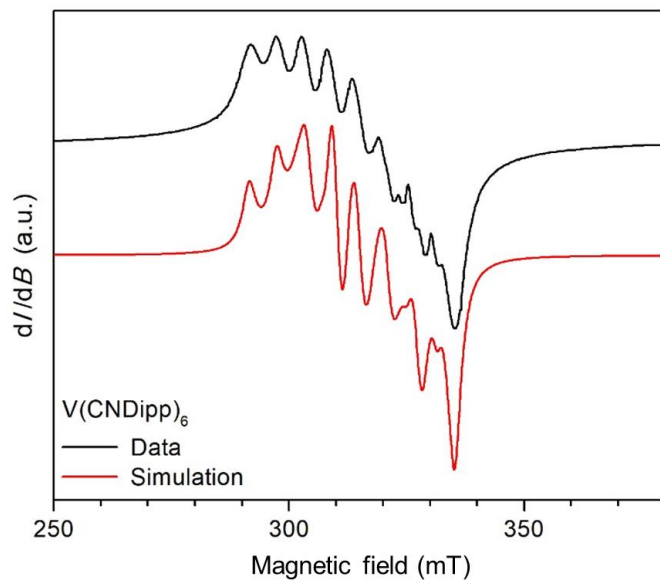


**Figure S7.** X-band EPR spectrum of  $V(CNDipp)_6$  (**1**) (black line) measured in a frozen toluene solution at 3 K using a microwave frequency of 9.099 GHz and simulation (red line).

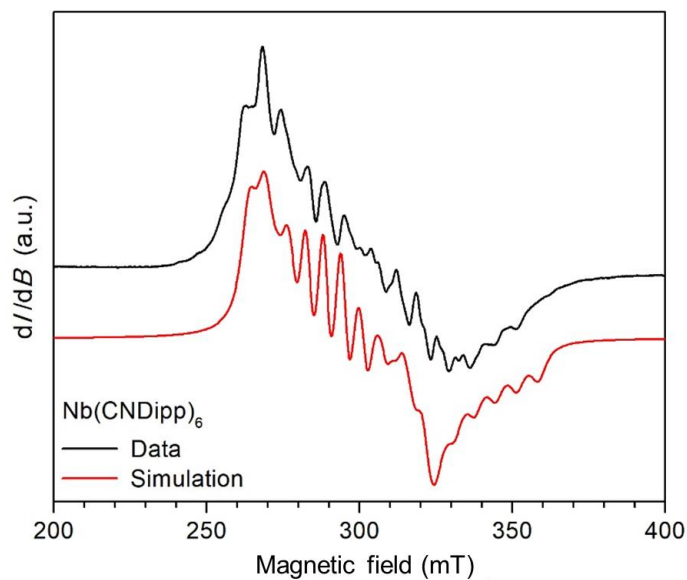


**Figure S8.** X-band EPR spectrum of  $Nb(CNDipp)_6$  (**2**) measured in a frozen toluene solution at 7 K using a microwave frequency of 9.216 GHz, field modulation amplitude 32 G at 100 kHz, microwave power 1 mW. Data are plotted as a black line and the simulation as a red line. Note the large modulation amplitude used in the measurement which might distort the spectrum.

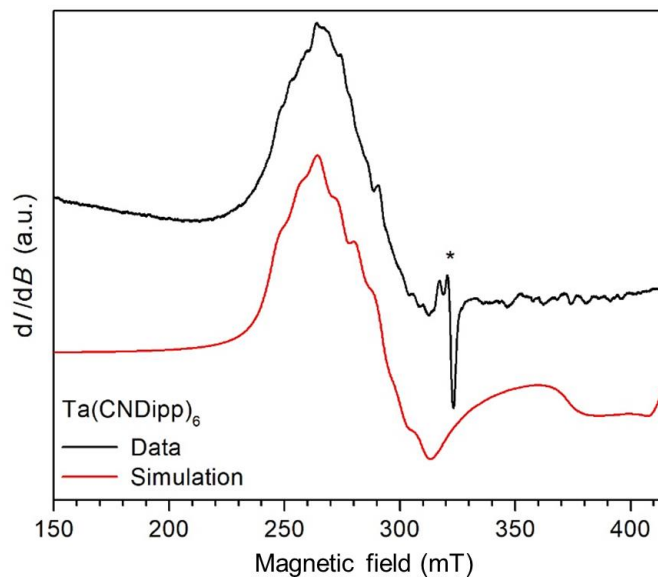


**Figure S9.** X-band EPR spectrum of  $\text{Ta}(\text{CNDipp})_6$  (**3**) measured in a frozen toluene solution at 15 K using a microwave frequency of 9.03 GHz, field modulation amplitude 32 G at 100 kHz, microwave power 10 mW. Data are plotted as a black line and the simulation as a red line. The asterisk denotes an isotropic  $S = 1/2$  impurity.

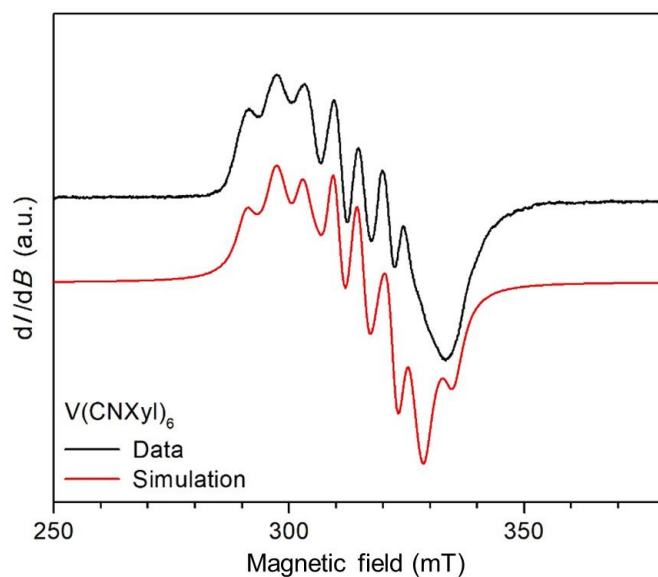


**Figure S10.** X-band EPR spectrum of  $\text{V}(\text{CNXyl})_6$  measured in a frozen toluene solution (1 mM) at 25 K using a microwave frequency of 9.225 GHz, field modulation amplitude 32 G at 100 kHz, microwave power 15  $\mu\text{W}$ . Data are plot as a black line and the simulation as a red line. Note the large modulation amplitude used in the measurement which might distort the spectrum.

**Table S5.** EPR simulation parameters for frozen solution spectra of **1–3**.

	V(CNDipp) <sub>6</sub> ( <b>1</b> )	Nb(CNDipp) <sub>6</sub> ( <b>2</b> )	Ta(CNDipp) <sub>6</sub> ( <b>3</b> )	V(CNXyl) <sub>6</sub>
$g_x$	2.079	2.215	2.33	2.105
$g_y$	2.079	2.215	2.33	2.105
$g_z$	2.002	1.97	1.64	2.07
$A_x$ (MHz)	82	160	120	110
$A_y$ (MHz)	172	200	290	185
$A_z$ (MHz)	85	180	130	30
Linewidth (mT)	2	3.5	7	3

## Magnetic Measurements

Microcrystalline samples of **1**, **2**, and **3** were loaded into 7 mm outer diameter (5 mm inner diameter) quartz tubes with a raised quartz platform. Glass wool was packed on top of each sample to restrain the samples. The quartz tubes were then briefly evacuated and flame sealed to protect the samples from air exposure. Alternatively, eicosane was added on top of the sample, the tube was evacuated and sealed, and the sample was briefly heated to 40 °C to melt the eicosane to restrain the sample. Magnetic susceptibility measurements were performed using a Quantum Design MPMS2 SQUID magnetometer. All dc susceptibility data were corrected for diamagnetic contributions from the compounds and from glass wool<sup>12</sup> or eicosane estimated using Pascal's constants.<sup>13</sup> Uncertainty analysis of the ac susceptibility parameters was performed using macro SolverAid implemented in Excel.<sup>14</sup> In the  $\chi_M T$  plot of **1** (Figure S11), a small upturn was observed below 18 K, which may be attributed to magnetic torquing due to imperfect sample restraint by glass wool. Steep  $\chi_M T$  downturns below ~5 K in all samples may be attributed to antiferromagnetic intermolecular interactions, which also manifest as exchange narrowing in the EPR spectra of solid samples.

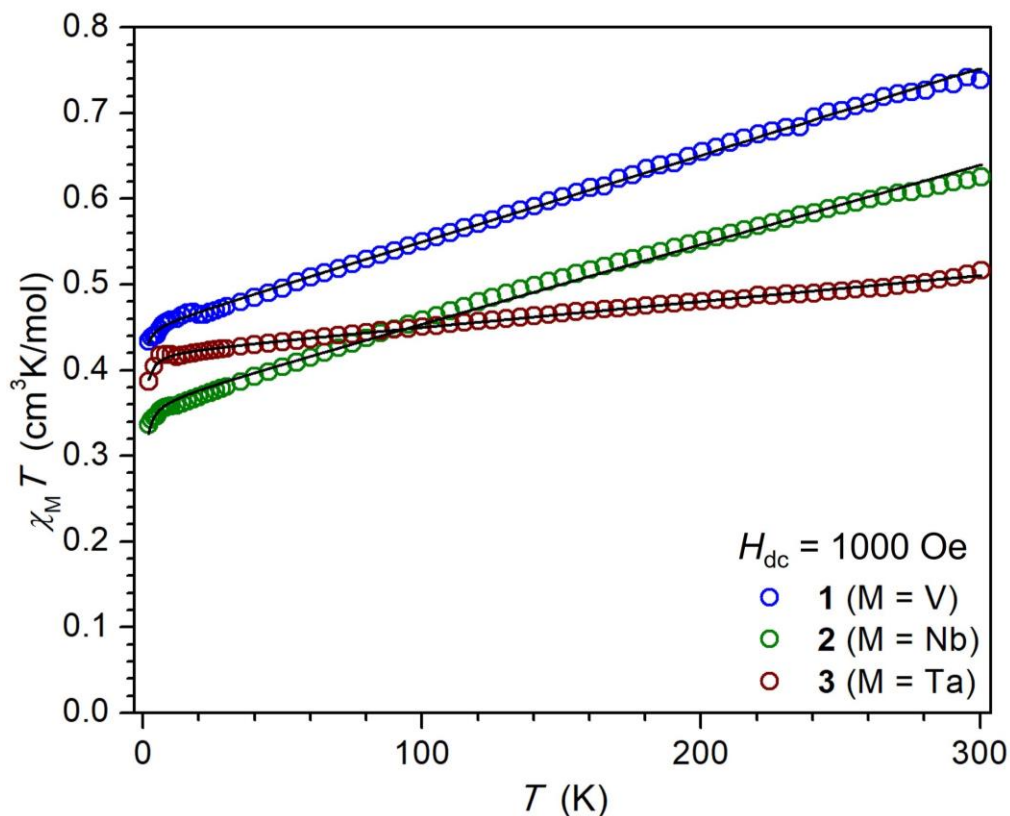


**Figure S11.** Variable-temperature  $\chi_M T$  data for V(CNDipp)<sub>6</sub> (**1**, blue circles), Nb(CNDipp)<sub>6</sub> (**2**, green circles), and Ta(CNDipp)<sub>6</sub> (**3**, dark red circles) measured under a 1000 Oe applied field. The data for **3** are reproduced from ref<sup>15</sup>. Black lines represent fits to the data. Fitting parameters: **1**,  $g_{\text{iso}} = 2.19$ ,  $\chi_{\text{TIP}} = 1.01 \times 10^{-3} \text{ cm}^3/\text{mol}$ ,  $zJ = -0.053 \text{ cm}^{-1}$ ; **2**,  $g_{\text{iso}} = 1.97$ ,  $\chi_{\text{TIP}} = 9.26 \times 10^{-4} \text{ cm}^3/\text{mol}$ ,  $zJ = -0.168 \text{ cm}^{-1}$ ; **3**,  $g_{\text{iso}} = 2.12$ ,  $\chi_{\text{TIP}} = 3.01 \times 10^{-4} \text{ cm}^3/\text{mol}$ ,  $zJ = -0.102 \text{ cm}^{-1}$ , where  $zJ$  is the mean intermolecular interactions.

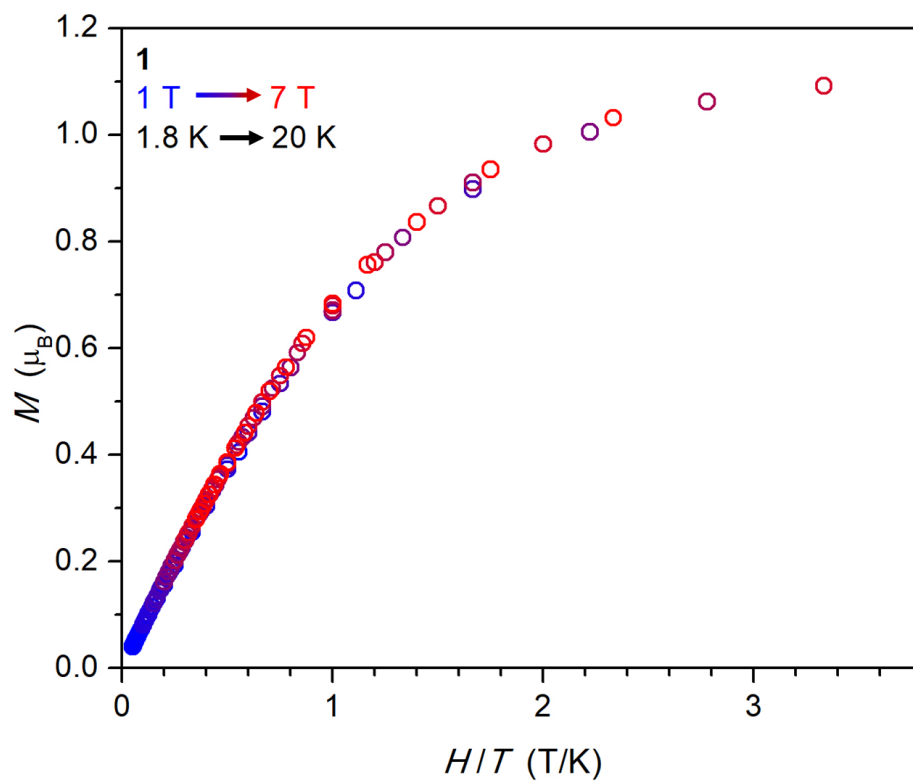


**Figure S12.** Reduced magnetization data for  $V(\text{CNDipp})_6$  (**1**) collected under fields of 1 to 7 T from 1.8 to 20 K.



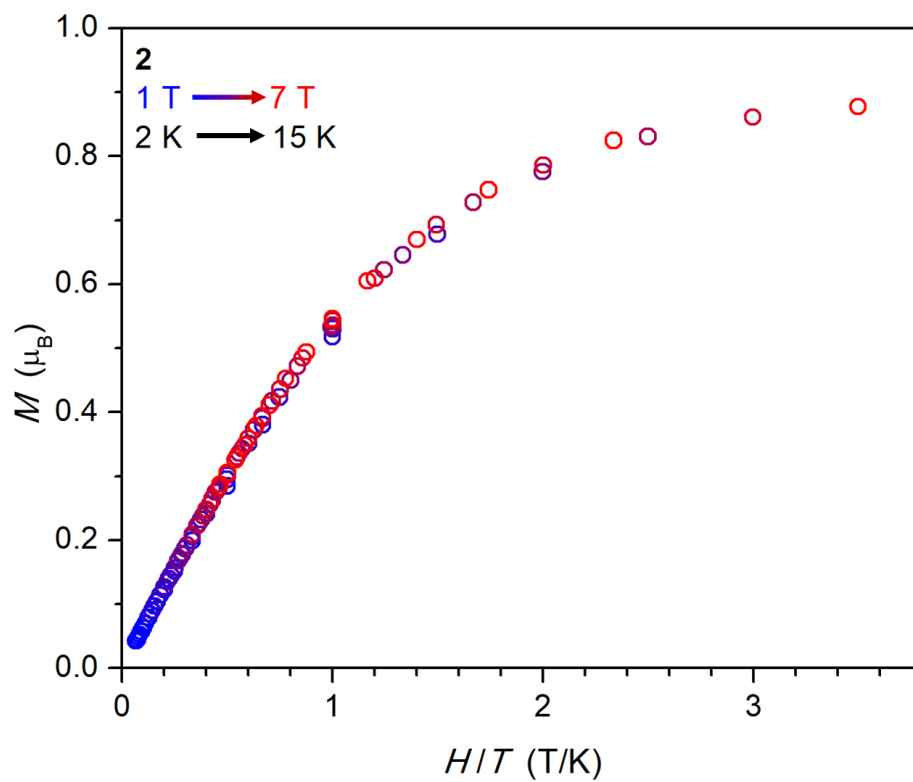


**Figure S13.** Reduced magnetization data for Nb(CNDipp)<sub>6</sub> (**2**) collected under fields of 1 to 7 T from 2 to 15 K.

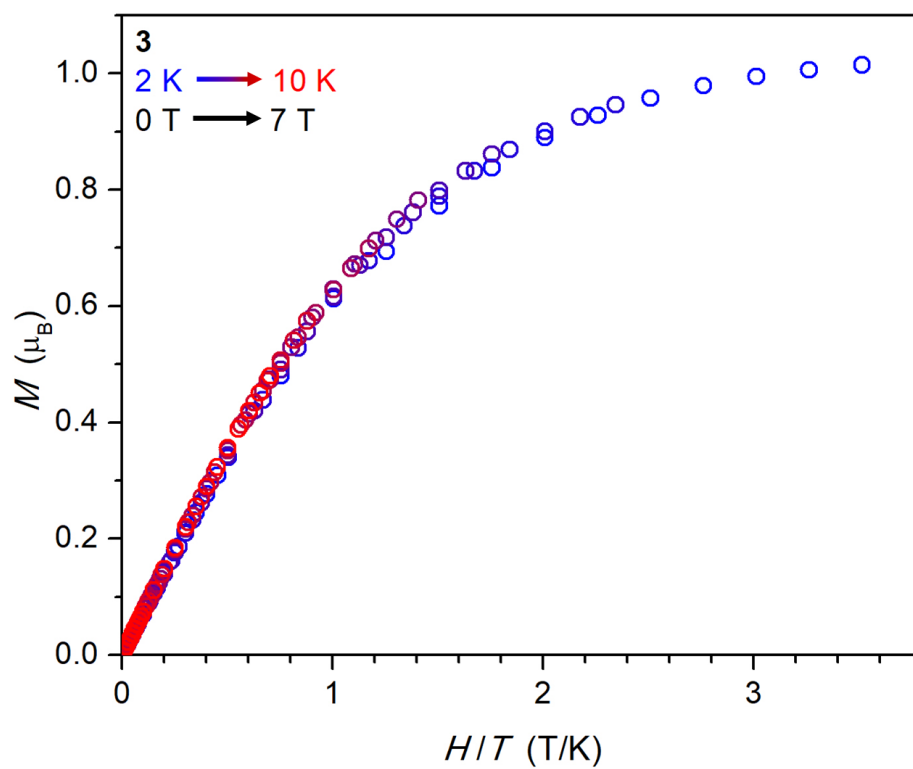


**Figure S14.** Reduced magnetization data for Ta(CNDipp)<sub>6</sub> (**3**) collected under fields of 0 to 7 T from 2 to 10 K.

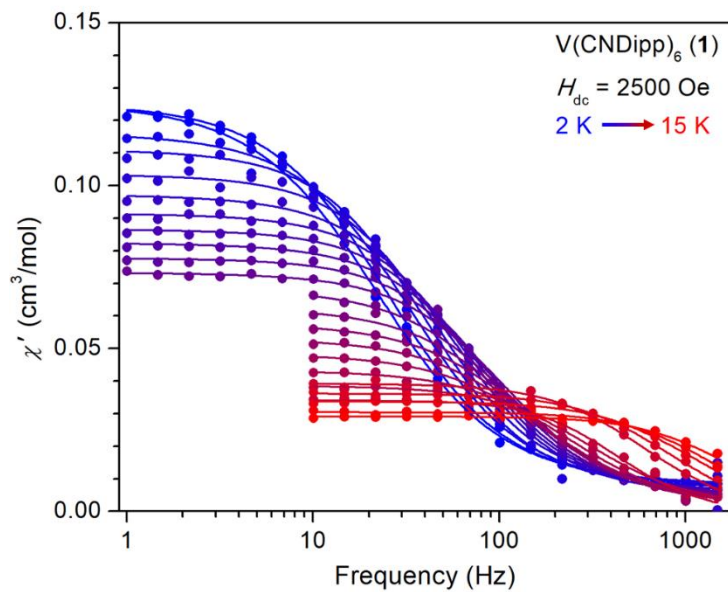


**Figure S15.** Variable-temperature, variable-frequency in-phase components of the ac magnetic susceptibility data of **1** collected under a 2500 Oe applied magnetic field. Solid lines are fits to the data using a generalized Debye model.

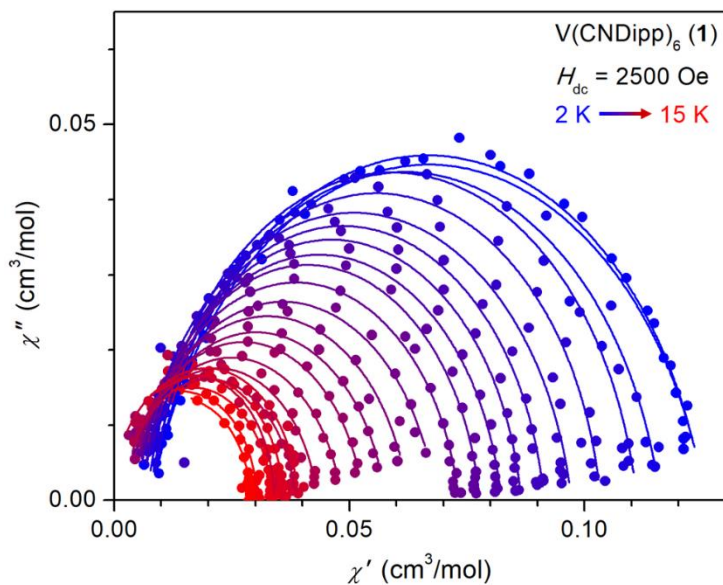


**Figure S16.** Variable-temperature Cole-Cole plots for **1** collected under a 2500 Oe applied field. Solid lines represent fits to the data using a generalized Debye model.

**Table S6.** Fitting parameters for the variable-temperature, variable-frequency ac susceptibility data for **1** under an applied field of 2500 Oe.

$T$ (K)	$\chi_T$ (cm <sup>3</sup> /mol)	$\chi_S$ (cm <sup>3</sup> /mol)	$\alpha$	$\tau$ (ms)	Residual ( $\times 10^{-5}$ )
2.00	0.1258(6)	0.0079(5)	0.166(7)	7.1(1)	4.55
2.25	0.1255(9)	0.0080(7)	0.15(1)	6.3(1)	9.38
2.50	0.116(1)	0.007(1)	0.13(1)	4.7(1)	16.7
2.75	0.1112(8)	0.0070(8)	0.10(1)	3.98(9)	11.2
3.00	0.1035(7)	0.0080(8)	0.09(1)	3.34(7)	9.94
3.25	0.0972(6)	0.0048(8)	0.11(1)	2.70(6)	8.65
3.50	0.0914(4)	0.0060(5)	0.089(8)	2.40(3)	2.96
3.75	0.0865(3)	0.0058(4)	0.086(8)	2.11(3)	2.58
4.00	0.0823(3)	0.0048(5)	0.098(8)	1.86(3)	2.81
4.25	0.0777(4)	0.0046(5)	0.088(9)	1.72(3)	3.21
4.60	0.0733(4)	0.0040(7)	0.10(1)	1.50(3)	4.78
5.00	0.0683(6)	0.0035(6)	0.12(1)	1.42(3)	1.76
5.50	0.0625(7)	0.0027(7)	0.12(2)	1.26(4)	3.00
6.00	0.0577(6)	0.0027(7)	0.12(2)	1.14(3)	2.15
6.50	0.0530(5)	0.0018(5)	0.11(1)	1.02(2)	1.33
7.20	0.0484(6)	0.0016(7)	0.12(2)	0.87(3)	2.23
8.00	0.0432(5)	0.0010(8)	0.11(2)	0.67(3)	2.46
9.00	0.0385(3)	0.0017(5)	0.07(1)	0.52(1)	0.69
10.00	0.0340(6)	0	0	0.37(2)	9.31
11.00	0.0392(2)	0	0.06(1)	0.267(4)	0.84
12.00	0.0361(1)	0	0.046(7)	0.199(2)	0.33
13.00	0.0337(2)	0	0.06(1)	0.149(3)	0.88
14.00	0.0304(2)	0	0.02(2)	0.117(3)	1.07
15.00	0.0291(2)	0	0.04(2)	0.093(2)	0.64

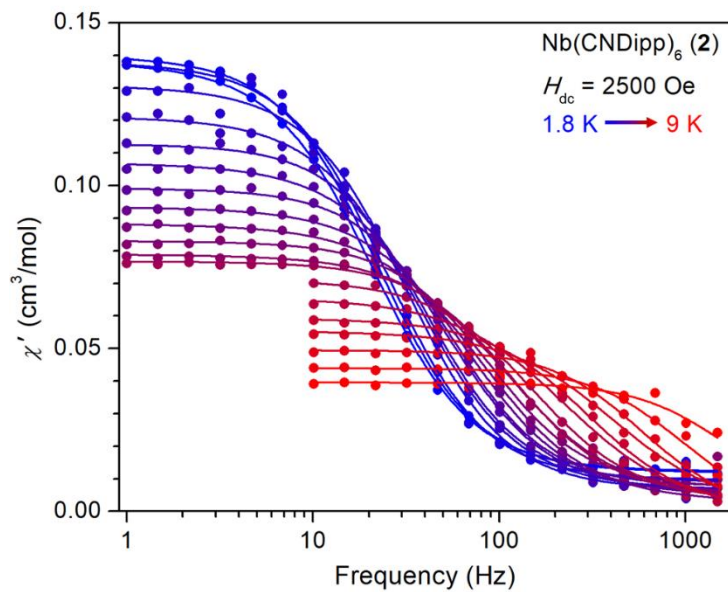


**Figure S17.** Variable-temperature, variable-frequency in-phase components of the ac magnetic susceptibility data for **2** collected under a 2500 Oe applied magnetic field. Solid lines are fits to the data using a generalized Debye model.

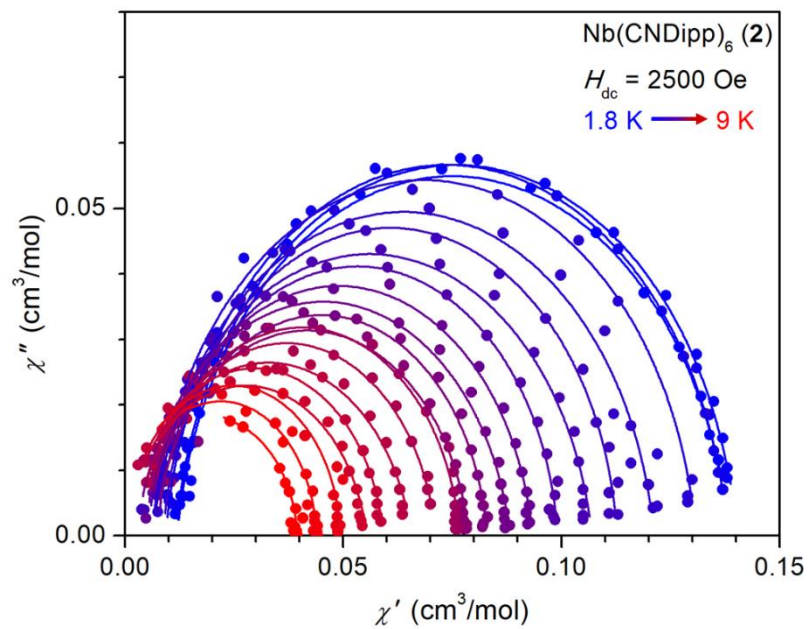


**Figure S18.** Variable-temperature Cole-Cole plots for **2** collected under a 2500 Oe applied field. Solid lines represent fits to the data using a generalized Debye model.

**Table S7.** Fitting parameters for the variable-temperature, variable-frequency ac susceptibility data of **2** under an applied field of 2500 Oe.

$T$ (K)	$\chi_T$ (cm <sup>3</sup> /mol)	$\chi_S$ (cm <sup>3</sup> /mol)	$\alpha$	$\tau$ (ms)	Residual ( $\times 10^{-5}$ )
1.80	0.1368(4)	0.0112(4)	0.075(6)	7.64(8)	6.45
2.00	0.1388(4)	0.0108(4)	0.067(6)	7.19(7)	6.41
2.25	0.1379(4)	0.0094(5)	0.069(6)	6.47(7)	7.64
2.50	0.1307(8)	0.007(1)	0.07(1)	5.1(1)	28.8
2.75	0.1213(4)	0.0065(5)	0.083(7)	4.38(6)	7.16
3.00	0.1128(4)	0.0088(6)	0.051(9)	3.92(6)	9.40
3.25	0.1070(5)	0.0050(5)	0.097(8)	3.19(4)	4.37
3.50	0.0992(4)	0.0075(5)	0.057(7)	2.86(4)	3.46
3.75	0.0934(3)	0.0045(4)	0.086(7)	2.34(3)	2.55
4.00	0.0883(5)	0.0026(7)	0.10(1)	1.96(4)	6.05
4.25	0.0830(3)	0.0071(5)	0.063(9)	1.78(3)	3.08
4.50	0.0788(5)	0.0046(7)	0.10(1)	1.42(3)	5.48
4.60	0.0768(3)	0.0043(6)	0.07(1)	1.33(2)	3.26
5.00	0.0712(5)	0.0028(5)	0.09(1)	1.03(2)	1.45
5.50	0.066(1)	0	0.13(2)	0.70(3)	8.77
6.00	0.0592(5)	0	0.08(1)	0.53(1)	2.43
6.50	0.0554(7)	0	0.11(2)	0.38(1)	5.39
7.20	0.0494(5)	0	0.03(2)	0.273(7)	3.42
8.00	0.0439(4)	0	0.03(2)	0.170(4)	2.45
9.00	0.0395(4)	0	0.05(2)	0.091(4)	2.73

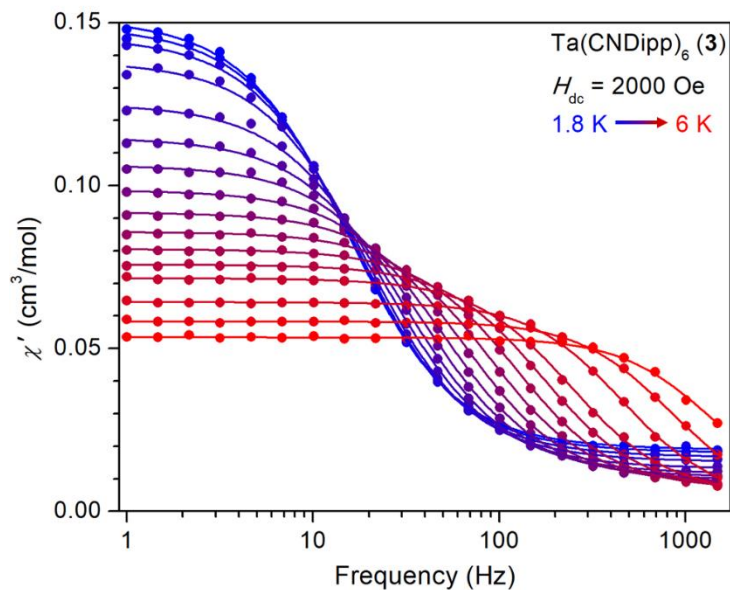


**Figure S19.** Variable-temperature, variable-frequency in-phase components of the ac magnetic susceptibility data for **3** collected under a 2000 Oe applied magnetic field. Solid lines are fits to the data using a generalized Debye model.

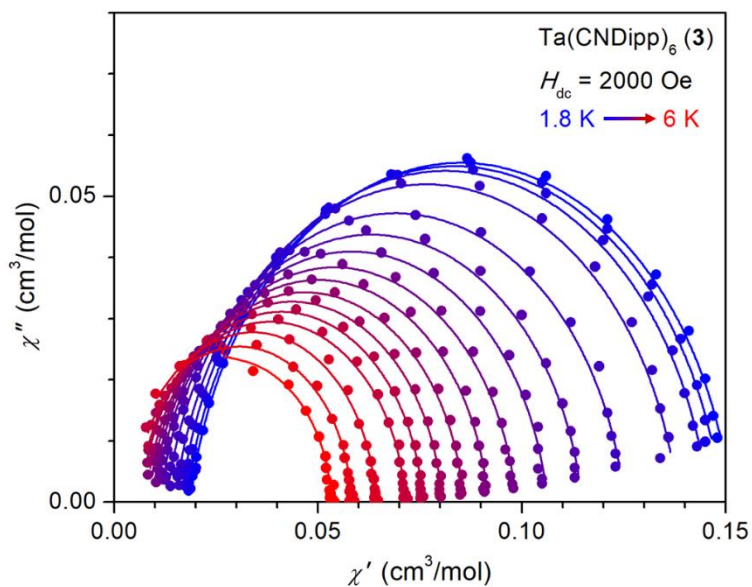


**Figure S20.** Variable-temperature Cole-Cole plots for **3** collected under a 2000 Oe applied field. Solid lines represent fits to the data using a generalized Debye model.

**Table S8.** Fitting parameters for the variable-temperature, variable-frequency ac susceptibility data for **3** under an applied field of 2000 Oe.

$T$ (K)	$\chi_T$ (cm <sup>3</sup> /mol)	$\chi_S$ (cm <sup>3</sup> /mol)	$\alpha$	$\tau$ (ms)	Residual ( $\times 10^{-5}$ )
1.80	0.1514(3)	0.0187(2)	0.103(3)	10.36(6)	1.14
1.90	0.1491(4)	0.0178(3)	0.103(4)	9.89(7)	1.75
2.00	0.1458(3)	0.0164(2)	0.103(3)	9.29(5)	0.84
2.25	0.1383(4)	0.0150(3)	0.098(5)	8.18(7)	2.16
2.50	0.1253(3)	0.0129(3)	0.099(4)	6.45(5)	1.71
2.75	0.1148(3)	0.0114(2)	0.096(4)	5.14(3)	1.23
3.00	0.1063(3)	0.0103(3)	0.090(5)	4.08(3)	1.40
3.25	0.0986(2)	0.0094(3)	0.085(5)	3.16(3)	1.18
3.50	0.0918(2)	0.0086(3)	0.074(5)	2.39(2)	1.13
3.75	0.0858(2)	0.0078(3)	0.070(5)	1.77(1)	0.87
4.00	0.0805(2)	0.0068(3)	0.063(5)	1.29(1)	0.84
4.25	0.0757(1)	0.0062(2)	0.059(4)	0.926(6)	0.44
4.50	0.0716(2)	0.0050(4)	0.065(6)	0.655(6)	0.79
5.00	0.0642(1)	0.0038(4)	0.041(6)	0.348(4)	0.59
5.50	0.05828(8)	0.0032(5)	0.038(6)	0.192(2)	0.29
6.00	0.0534(1)	0.002(1)	0.04(1)	0.111(4)	0.78



## Relaxation Dynamics

Relaxation times for **1–3** were fit using Eq. (1) in the manuscript. At least two phonon modes were required to fit the data across the whole temperature range. Low temperature region was fit with an inclusion of a quantum tunneling of magnetization process. Therefore, the relaxation times are described by the following equation:

$$\tau^{-1} = \frac{V_1^2}{\hbar\omega_1} \exp\left(-\frac{\hbar\omega_1}{2k_B T}\right) + \frac{V_2^2}{\hbar\omega_2} \exp\left(-\frac{\hbar\omega_2}{2k_B T}\right) + \tau_{\text{QTM}}^{-1}$$

$$\tau^{-1} = \frac{V_1^2}{hc\tilde{\nu}_1} \exp\left(-\frac{hc\tilde{\nu}_1}{2k_B T}\right) + \frac{V_2^2}{hc\tilde{\nu}_2} \exp\left(-\frac{hc\tilde{\nu}_2}{2k_B T}\right) + \tau_{\text{QTM}}^{-1}$$

where  $V$  is the spin-vibronic coupling strength,  $\tilde{\nu}$  is phonon wavenumber,  $c$  is speed of light,  $\tau_{\text{QTM}}$  is the relaxation time of quantum tunneling process, and subscripts 1 and 2 denote the first and second phonon modes.

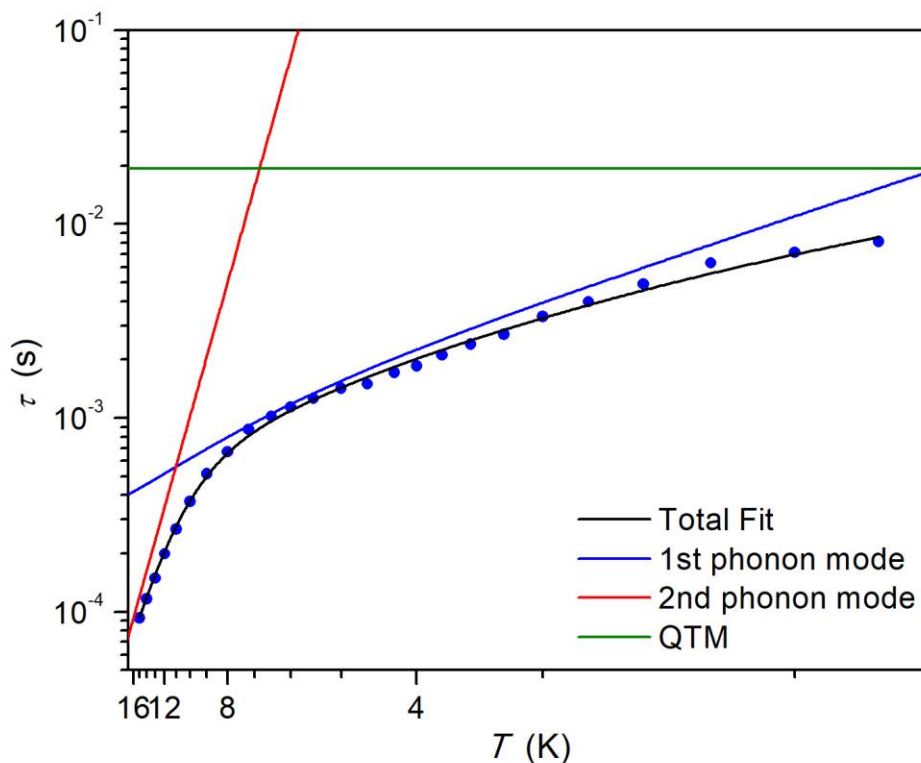


**Figure S21.** Arrhenius plot of relaxation time of  $\text{V}(\text{CNDipp})_6$  (**1**) measured under an optimized applied field of 2500 Oe. Error bars representing one standard deviation in the relaxation times are within the height of the data points. Red, blue, and green lines represent the first and second phonon modes and quantum tunnelling of magnetization contribution to the relaxation times. Black line represents the overall fit to the data. Fitting parameters:  $\tilde{\nu}_1 = 89(6) \text{ cm}^{-1}$ ,  $V_1 = 1.7(3) \times 10^{-2} \text{ cm}^{-1}$ ,  $\tilde{\nu}_2 = 8(1) \text{ cm}^{-1}$ ,  $V_2 = 2.8(5) \times 10^{-4} \text{ cm}^{-1}$ ,  $\tau_{\text{QTM}} = 19(9) \text{ ms}$ .

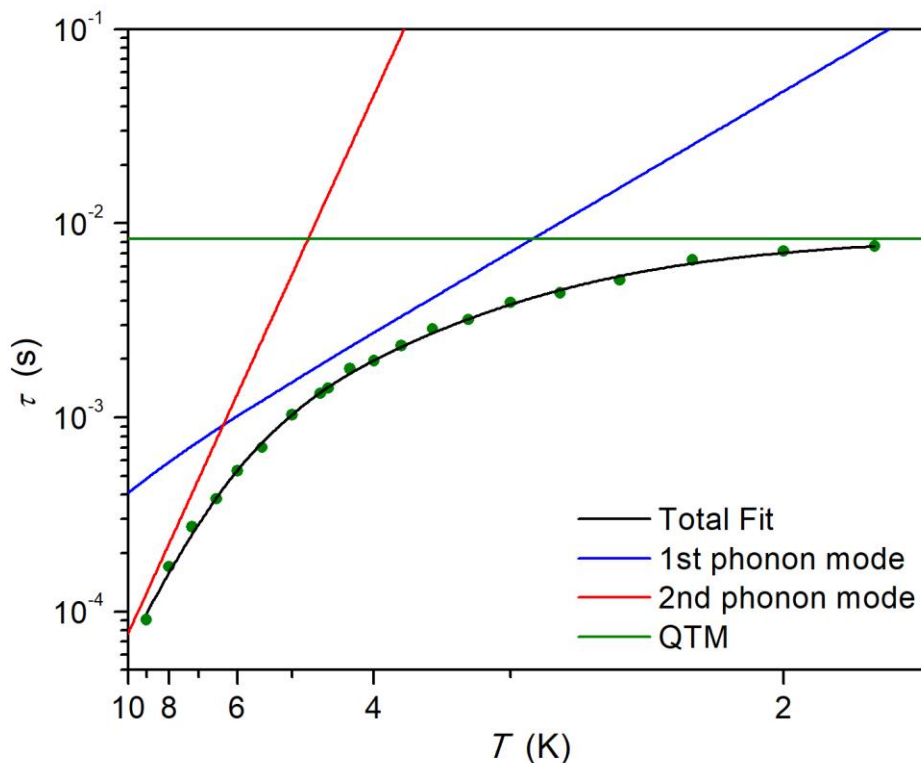


**Figure S22.** Arrhenius plot of relaxation time of Nb(CNDipp)<sub>6</sub> (**2**) measured under a 2500 Oe applied field. Error bars representing one standard deviation in the relaxation times are within the height of the data points. Red, blue, and green lines represent the first and second phonon modes and quantum tunnelling of magnetization contribution to the relaxation times. Black line represents the overall fit to the data. Best fitting parameters:  $\tilde{\nu}_1 = 59(4) \text{ cm}^{-1}$ ,  $V_1 = 1.7(3) \times 10^{-2} \text{ cm}^{-1}$ ,  $\tilde{\nu}_2 = 16(1) \text{ cm}^{-1}$ ,  $V_2 = 7(1) \times 10^{-4} \text{ cm}^{-1}$ ,  $\tau_{\text{QTM}} = 8.3(5) \text{ ms}$ .

Fitting the relaxation times of **2** and **3** involves significant uncertainties as there is a wide temperature range where both phonon modes contribute significantly to the total relaxation time. This causes a correlated change between  $\tilde{\nu}$  and  $V$ , resulting in several local minima with similar error residuals. Table S9 shows examples of three local minima in fitting the relaxation times of **2**. This ambiguity precludes determination of  $V$  without the knowledge of phonon frequencies.

**Table S9.** Example fitting parameters for relaxation times of **2**.

	Fit 1	Fit 2	Fit 3
$\tilde{\nu}_1 \text{ (cm}^{-1}\text{)}$	52(4)	59(4)	66(5)
$V_1 \text{ (cm}^{-1}\text{)}$	$1.2(2) \times 10^{-2}$	$1.7(3) \times 10^{-2}$	$2.4(6) \times 10^{-2}$
$\tilde{\nu}_2 \text{ (cm}^{-1}\text{)}$	14(2)	16(1)	17(1)
$V_2 \text{ (cm}^{-1}\text{)}$	$5.6(15) \times 10^{-4}$	$7(1) \times 10^{-4}$	$8(1) \times 10^{-4}$
$\tau_{\text{QTM}} \text{ (ms)}$	8.7(8)	8.3(5)	8.1(4)
Least square residual	$4.37 \times 10^{-2}$	$3.48 \times 10^{-2}$	$3.93 \times 10^{-2}$

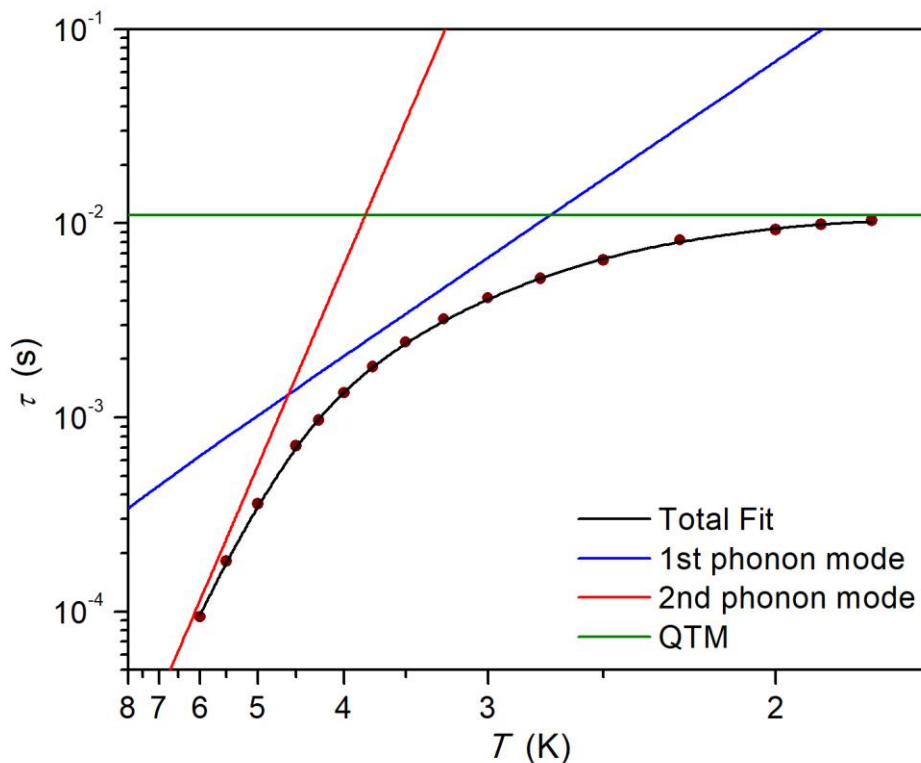


**Figure S23.** Arrhenius plot of relaxation time of Ta(CNDipp)<sub>6</sub> (**3**) measured under a 2000 Oe applied field. Error bars representing one standard deviation in the relaxation times are within the height of the data points. Red, blue, and green lines represent the first and second phonon modes and quantum tunnelling of magnetization contribution to the relaxation times. Black line represents the overall fit to the data. Best fitting parameters:  $\tilde{\nu}_1 = 66(2) \text{ cm}^{-1}$ ,  $V_1 = 9(1) \times 10^{-2} \text{ cm}^{-1}$ ,  $\tilde{\nu}_2 = 19.4(7) \text{ cm}^{-1}$ ,  $V_2 = 1.3(1) \times 10^{-3} \text{ cm}^{-1}$ ,  $\tau_{\text{QTM}} = 11.0(2) \text{ ms}$ .

**Table S10.** Best fitting parameters for relaxation times of **1–3**.

	<b>1</b>	<b>2</b>	<b>3</b>
$\tilde{\nu}_1 \text{ (cm}^{-1}\text{)}$	89(6)	59(4)	66(2)
$V_1 \text{ (cm}^{-1}\text{)}$	$1.7(3) \times 10^{-2}$	$1.7(3) \times 10^{-2}$	$9(1) \times 10^{-2}$
$\tilde{\nu}_2 \text{ (cm}^{-1}\text{)}$	8(1)	16(1)	19.4(7)
$V_2 \text{ (cm}^{-1}\text{)}$	$2.8(5) \times 10^{-4}$	$7(1) \times 10^{-4}$	$1.3(1) \times 10^{-3}$
$\tau_{\text{QTM}} \text{ (ms)}$	19(9)	8.3(5)	11.0(2)
Least square residual	$6.69 \times 10^{-2}$	$3.48 \times 10^{-2}$	$3.76 \times 10^{-3}$

## Density Functional Theory Calculations

The presence of a whole ligand disorder did not allow the use of the geometries as provided by the crystallographic CIF files in the calculation of their electronic structure and properties. A geometry optimization was needed beforehand. DFT geometry optimizations for  $M(\text{CNDipp})_6$  ( $M = \text{V}, \text{Nb}, \text{Ta}$ ) were performed using B3LYP functional and the D3BJ method to account for non-bonding interactions. Douglas-Kroll-Hess scalar relativistic method (DKH2) along with DKH-def2-SVP basis was used for all elements except for the transition metals, where DKH-def2-TZVP basis set was used for V, and SARC-DKH-TZVP basis set was used for Nb and Ta atoms.

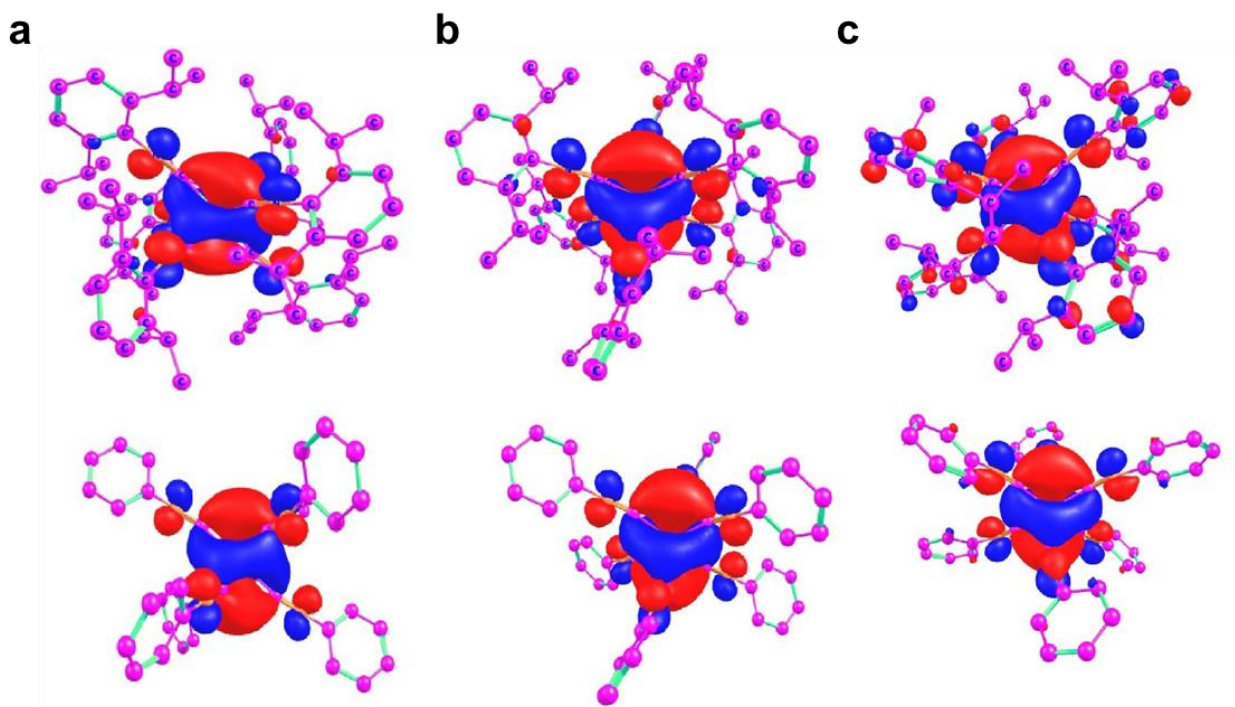


**Figure S24.** Contour plots of the molecular orbitals which carry the magnetic electron in  $\text{V}(\text{CNDipp})_6$  (**a**),  $\text{Nb}(\text{CNDipp})_6$  (**b**) and  $\text{Ta}(\text{CNDipp})_6$  (**c**) from Kohn-Sham DFT (top) and CASSCF (bottom); the increase of delocalization of the  $S = 1/2$  spin when going from  $\text{V}(\text{CNDipp})_6$  and  $\text{Nb}(\text{CNDipp})_6$  to  $\text{Ta}(\text{CNDipp})_6$  is best reflected by the DFT plot (**c**, top); contour values for the plot were set to 0.02 electron/Bohr<sup>3</sup>.

## Correlated Electronic Calculations

### 1. Sublevels of the $^2T_{2g}$ ground state

As a first step we attempted a classical ligand field calculation distributing five d electrons in the valence shell of the transition metal (CAS(5,5) active space). In these calculations we used DFT truncated model complexes,  $M(\text{CNPh})_6$ , (CNPh = phenylisocyanide, optimized geometries are included at the end of this document). Any attempt to localize and identify the d electrons on the transition metal using a CAS(5,5) active space failed. It turned out, that extended active spaces should be used involving external (empty) orbitals. The efforts getting CASSCF convergence resulted in a CAS(5,12) active space. The reason for this is best illustrated in Figure S25 showing orbitals from CASSCF converged calculation for  $\text{Ta}(\text{CNPh})_6$ . The molecular orbital (MO) plot shows Ta–C  $\pi$ -bonding and Ta–C  $\pi$ -antibonding partner MOs with the single spin residing on a bonding  $5d_{z^2}$  MO at lower energy and the corresponding empty Ta–C antibonding MO at higher energy. The figure illustrates the  $\pi$ -backbonding nature of the complex with the formally zero-valent Ta and a half-half sharing of the Ta  $5d_{z^2}$  orbital with the  $\pi^*$  orbital on CNPh. It is this electron sharing which renders the ligand field model inapplicable to the considered complexes.

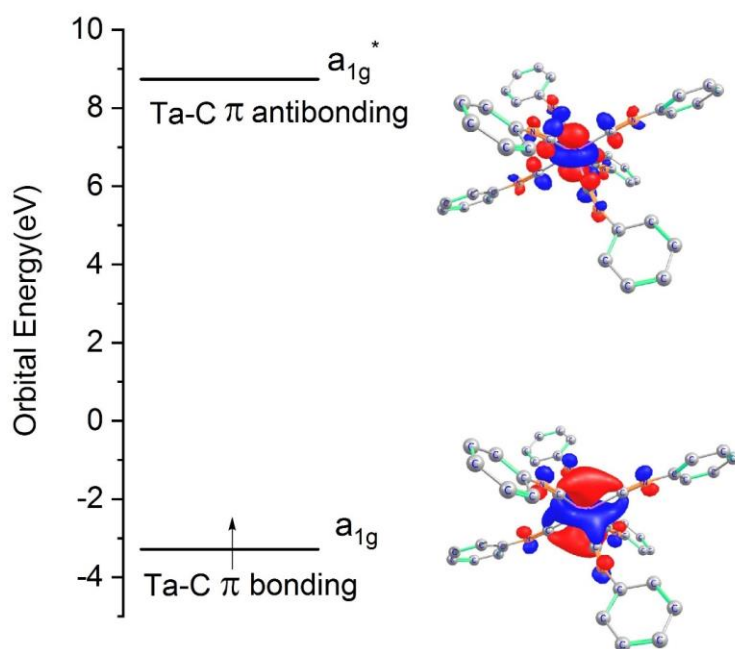


**Figure S25.** Ta–C  $\pi$ -bonding and Ta–C  $\pi$ -antibonding partner molecular orbitals of  $\text{Ta}(\text{CNPh})_6$  from CASSCF calculations with the single spin on the bonding, nominally  $5d_{z^2}$  orbital of Ta. The figure illustrates the  $\pi$ -backbonding nature of the complex with the formally zero-valent Ta. An electron density contour was plot at 0.04 electron/Bohr<sup>3</sup> to highlight the in-phase (bonding) and out-of-phase(antibonding) Ta–C combination of the metal  $5d_{z^2}$  and the ligand  $\pi^*$  orbital.

**Table S11.** Energies (eV), symmetry labels (pertaining to  $D_{3d}$  ( $O_h$ ) pseudo symmetry), Natural Orbital Occupations and percentage of metal d character of  $\pi$ -bonding and  $\pi$ -antibonding active MOs from converged CASSCF calculations of the  $M(\text{CNPh})_6$  ( $M = \text{V}, \text{Nb}, \text{Ta}$ ; CNPh = phenylisocyanide) series.

V(CNPh) <sub>6</sub>						
MO number	171	172	173	174	175	176
Symmetry	$e_g(t_{2g})$	$e_g(t_{2g})$	$a_{1g}(t_{2g})$	$e_g(t_{2g})$	$e_g(t_{2g})$	$a_{1g}(t_{2g})$
Energy (eV)	-3.18	-3.18	-3.13	8.92	8.92	9.18
$E(a_{1g})-E(e_g)$ (cm <sup>-1</sup> )	403			2097		
$N_{\text{occ}}$	1.58	1.58	1.58	0.08	0.08	0.08
%(3d)	57	57	62	59	59	59
Nb(CNPh) <sub>6</sub>						
MO number	180	181	182	184	185	183
Symmetry	$e_g(t_{2g})$	$e_g(t_{2g})$	$a_{1g}(t_{2g})$	$e_g(t_{2g})$	$e_g(t_{2g})$	$a_{1g}(t_{2g})$
Energy(eV)	-3.32	-3.32	-3.18	8.69	8.69	9.05
$E(a_{1g})-E(e_g)$ (cm <sup>-1</sup> )	1129			2903		
$N_{\text{occ}}$	1.63	1.63	1.62	0.04	0.04	0.04
%(4d)	52	52	56	57	57	57
Ta(CNPh) <sub>6</sub>						
MO number	197	198	196	200	201	199
Symmetry	$e_g(t_{2g})$	$e_g(t_{2g})$	$a_{1g}(t_{2g})$	$e_g(t_{2g})$	$e_g(t_{2g})$	$a_{1g}(t_{2g})$
Energy(eV)	-3.48	-3.48	-3.28	9.22	9.22	8.74
$E(a_{1g})-E(e_g)$ (cm <sup>-1</sup> )	1613			-3871		
$N_{\text{occ}}$	1.64	1.64	1.64	0.03	0.03	0.03
%(5d)	49	49	35	41	41	60

**Table S12.** Nonrelativistic (spin-free) and relativistic (spin-orbit coupled) states split out from the low-spin parent octahedral  $T_{2g}(d^5)$  ground state of DFT-optimized truncated model complexes  $M(\text{CNPh})_6$  (CNPh = phenylisocyanide;  $M = \text{V, Nb, Ta}$ ) from CASSCF (extended CAS(5,12) active space) and CASSCF/NEVPT2 calculations. Computed  $g$ -factors for the  $\Gamma_{4g}(1)$ ,  ${}^2A_{1g}$  ( $D_{3d}$ -point symmetry notations) ground state Kramers doublet are listed and compared with values extracted from X-band EPR spectra (in brackets). Symmetry notations pertain to the trigonal  $D_{3d}$  ( ${}^2A_{1g}$ ,  ${}^2E_g$  spin free, non-relativistic states) and the  $D_{3d}^*$  double group ( $\Gamma_{4g}$ ,  $\Gamma_{5g}$ ,  $\Gamma_{6g}$  spin-orbit coupled) points groups.

	V(CNPh) <sub>6</sub>		Nb(CNPh) <sub>6</sub>		Ta(CNPh) <sub>6</sub>	
	CASSCF	CASSCF/ NEVPT2	CASSCF	CASSCF/ NEVPT2	CASSCF	CASSCF/ NEVPT2
${}^2A_{1g}$	0	0	0	0	0	0
${}^2E_g$	1912	2280	1902	2280	1143	1099
$\Gamma_{4g}$	0	0	0	0	0	0
$\Gamma_{5g}$	1874	2241	1826	2199	1380	1356
$\Gamma_{6g}$	1957	2324	2022	2398	1804	1770
$\zeta_{\text{eff}}$	81 (114) <sup>a</sup> [158] <sup>b</sup>		187 (375) <sup>a</sup> [475] <sup>b</sup>		378 (1538) <sup>a</sup> [1657] <sup>b</sup>	
$g_{\parallel}$	1.996 (2.002)	1.998 (2.002)	1.958 (1.966)	1.972 (1.966)	0.815 (1.642)	0.754 (1.642)
$g_{\perp}$	2.086 (2.065)	2.072 (2.065)	2.213 (2.168)	2.180 (2.168)	2.564 (2.372)	2.560 (2.372)

<sup>a</sup>free atom values obtained from CASSCF calculations; <sup>b</sup>reported in J.S.Griffith, The Theory of Transition-Metal Ions, Cambridge University Press, 1961, p.437-438.

## 2. Static Jahn-Teller effect

For an octahedron inscribed in a cube, four such isoenergetic minima with trigonal axes oriented along the body diagonals of the cube are possible (Figure S26). The trigonal mode which drives the octahedral complex to these minima is illustrated in Figure S27. Equation S1 describes in analytical form the trigonal distortion:

$$Q_{\tau} = (1/\sqrt{6})R(\delta\theta_1 + \delta\theta_2 + \delta\theta_3 - \delta\theta_4 - \delta\theta_5 - \delta\theta_6) \quad (\text{S1})$$

where  $R$  is the metal–ligand bond distance, and  $\delta\theta_i$  is the angular deviation of each ligand ( $i = 1$  to 6) away from its idealized value  $\theta_{Oh} = 54.735^\circ$  in an octahedral geometry.

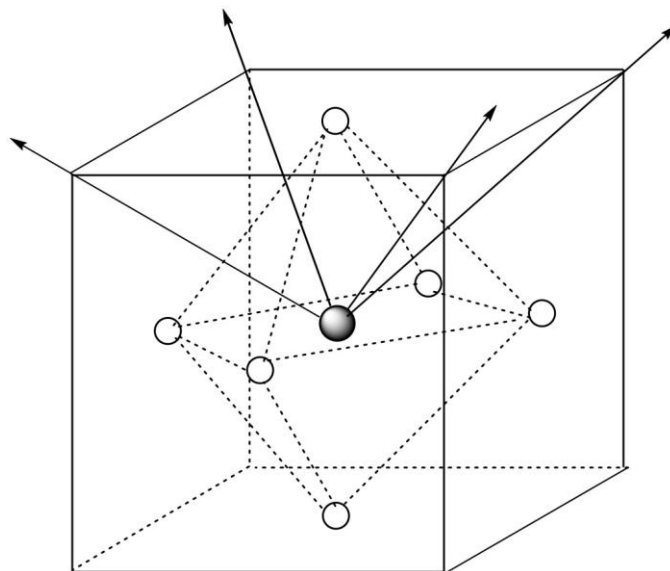


**Figure S26.** The hypothetical octahedral  $MC_6$  core of the  $M(\text{CNDipp})_6$  complexes inscribed in a cube; arrows along the body the diagonals of the cube show the trigonal axes of the four possible distorted structures with  $D_{3d}$  symmetry corresponding to the trigonal component ( $\alpha_{1g}$ ) of the octahedral  $\tau_{2g}$  vibration. Vibronic coupling of the ground  ${}^2T_{2g}$  ( $O_h$ ) state to this vibration leads to minima or saddle points (depending on the sign) with trigonal  $D_{3d}$  symmetry. Only one of the minima can be stabilized as a result of the  ${}^2T_{2g} \otimes \tau_{2g}$  static Jahn-Teller effect representing the geometry and orientation of the trigonal axes in the crystal structures of  $M(\text{CNDipp})_6$ . The disorder of CNDipp ligand in the crystal structures of  $V(\text{CNDipp})_6$  and  $Nb(\text{CNDipp})_6$  might originate from a partial dynamics due to the possible inversion from one of the four minima in the ground state potential energy surface of the complex to a neighboring minimum. The absence of such disorder in the structure of  $Ta(\text{CNDipp})_6$  might be due to a weakening of the Jahn-Teller effect when going from  $V(\text{CNDipp})_6$  and  $Nb(\text{CNDipp})_6$  to  $Ta(\text{CNDipp})_6$ .



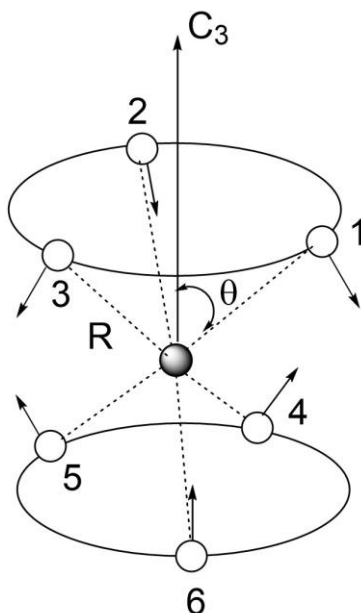


**Figure S27.** The trigonal effective interaction mode of  $t_{2g}(a_{1g})$   $O_h(D_{3d})$  point group symmetry, contributing to the trigonal compressions of the parent undistorted octahedral complexes as the result of the  ${}^2T_{2g} \otimes \tau_{2g}$  Jahn-Teller effect observed in the crystal structures of  $V(\text{CNDipp})_6$ ,  $\text{Nb}(\text{CNDipp})_6$  and  $\text{Ta}(\text{CNDipp})_6$ . The deviations of the polar angle ( $\theta \approx 58^\circ$ ) from the octahedral value ( $\theta_{Oh} = 54.735^\circ$ ) and the metal–ligand distance  $R$  used in the definition of the trigonal mode  $Q_\tau$  are shown.

Depending on the donor properties of the ligand, trigonally elongation,  $\delta\theta_i < 0$  ( $\pi$ -donor) or trigonally compression  $\delta\theta_i > 0$  ( $\pi$ -acceptor ligands) minima are possible. In either case, the stabilization of a non-degenerate  ${}^2A_{1g}$  ground state is the precondition for the distortion. In agreement with the  $\pi$ -backbonding character of the CNDipp ligands, trigonally compressed geometries in all three  $M(\text{CNDipp})_6$  complexes are observed. The theory of Jahn-Teller effect in  ${}^2T_{2g}$  states is rather involved but well elaborated,<sup>16,17</sup> and was previously applied in the study of hexacyano 3d transition metal complexes.<sup>18</sup> In the complexes considered here, Jahn-Teller distortions are static; out of the four minima only one is stabilized in solids state structures.<sup>†</sup>

In simple terms, the energies of  ${}^2A_{1g}$  and  ${}^2E_g$  states, split out from the  ${}^2T_{2g}$  octahedral ground state can be parametrized using a Harmonic energy term  $(1/2)K_\tau Q_\tau^2$  which represents the restoring force in an octahedral complex in a non-degenerate ground state and a linear vibronic term  $V_\tau Q_\tau$  which induces the splitting and lifts the orbital degeneracy:

$$E({}^2A_{1g}) = (1/2)K_\tau Q_\tau^2 - V_\tau Q_\tau \quad (\text{S2})$$

<sup>†</sup> The observation of a distorted structure for complex with  $O_h$  and a  ${}^2T_{2g}$  ground state in a solid does not necessarily imply a static Jahn-Teller mechanism; external perturbations from other ions in ionic solids with symmetries lower than cubic might mimic geometries not supported by the intrinsic Jahn-Teller effect. However, for the neutral complexes of the type discussed here, such effects are expected weak, to justify a Jahn-Teller interpretation of the observed geometries.

$$E(^2E_g) = (1/2)K_\tau Q_\tau^2 + (1/2)V_\tau Q_\tau \quad (\text{S3})$$

From the molecular structure, we extract the value of  $Q_\tau$  at the energy minimum ( $Q_\tau^o$ ). Using the  ${}^2E_g - {}^2A_{1g}$  energy splitting at the minimum, i.e. the energy of the purely electronic Frank-Condon transition at the minimum ( $\Delta E_{FC}^m$ , see Figure S28), it is possible to estimate the Jahn-Teller parameters: the harmonic force field constant,  $K_\tau$ , and the linear Jahn-Teller coupling constant,  $V_\tau$ :

$$V_\tau = (2/3)(\Delta E_{FC}^m / Q_\tau^o) \quad (\text{S4})$$

$$K_\tau = (2/3)(\Delta E_{FC}^m / (Q_\tau^o)^2) \quad (\text{S5})$$

Values of  $Q_\tau^o$ ,  $\Delta E_{FC}^m$ ,  $V_\tau$  and  $K_\tau$  deduced are collected in

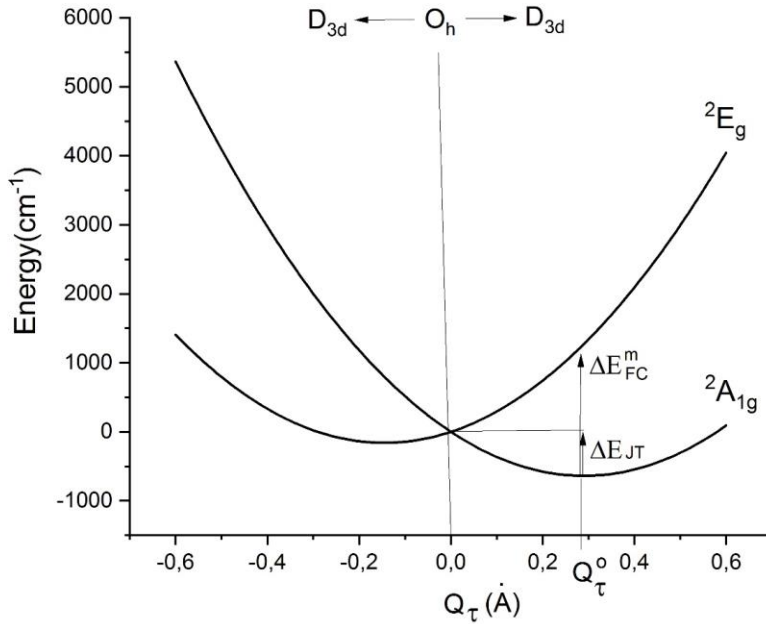


**Figure S28.** Energy dependence of the  ${}^2T_{2g}$  ground state of a (hypothetical) octahedral  $M(\text{CNPh})_6$  complex on the effective interacting Jahn-Teller active normal mode  $Q_\tau$  and visual definition of the parameters of the  ${}^2T_2 \otimes \tau$  Jahn-Teller problem: the Jahn-Teller stabilization energy ( $\Delta E_{JT}$ ), the energy of the vertical (Frank Condon) transition from the  $D_{3d} {}^2A_{1g}$  ground state minimum to the  ${}^2E_g$  excited state at the same geometry ( $\Delta E_{FC}^m$ ), and the value of the Jahn-Teller displacement ( $Q_\tau^o$ ). The plot was constructed using the values of the linear vibronic coupling constant ( $V_\tau$ ) and the harmonic force constant ( $K_\tau$ ) of  $V(\text{CNPh})_6$  (Table S13).

**Table S13.** The decrease of the linear vibronic coupling constant across the series,  $V_\tau = 4395$  (V), 3474 (Nb) and 2920  $\text{cm}^{-1}/\text{\AA}$  (Ta) reflects a weakening of vibronic coupling, just opposite to the increase of the effective spin-orbit coupling constant. We note in the next section that this weakening might dampen the effect of increased spin-orbit coupling on spin relaxation time.

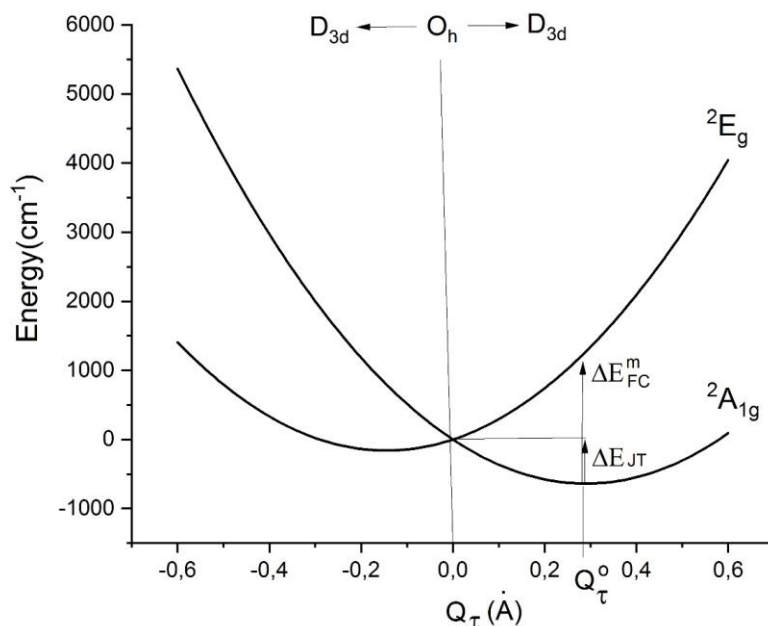


**Figure S28.** Energy dependence of the  ${}^2T_{2g}$  ground state of a (hypothetical) octahedral  $M(\text{CNPh})_6$  complex on the effective interacting Jahn-Teller active normal mode  $Q_\tau$  and visual definition of the parameters of the  ${}^2T_2 \otimes \tau$  Jahn-Teller problem: the Jahn-Teller stabilization energy ( $\Delta E_{JT}$ ), the energy of the vertical (Frank Condon) transition from the  $D_{3d}$   ${}^2A_{1g}$  ground state minimum to the  ${}^2E_g$  excited state at the same geometry ( $\Delta E_{FC}^m$ ), and the value of the Jahn-Teller displacement ( $Q_\tau^0$ ). The plot was constructed using the values of the linear vibronic coupling constant ( $V_\tau$ ) and the harmonic force constant ( $K_\tau$ ) of  $V(\text{CNPh})_6$  (Table S13).

**Table S13.** Jahn-Teller parameters deduced using DFT optimized geometries of truncated  $M(\text{CNPh})_6$  (CNPh = phenylisocyanide;  $M = \text{V}, \text{Nb}, \text{Ta}$ ) model complexes and CASSCF computed  ${}^2T_{2g} \rightarrow {}^2A_{1g}$  (ground state) +  ${}^2E_g$  (excited state, see Table S12) Jahn-Teller splitting using CAS(5,12) active spaces.

	$V(\text{CNPh})_6$	$\text{Nb}(\text{CNPh})_6$	$\text{Ta}(\text{CNPh})_6$
$Q_\tau^0$ (exp) ( $\text{\AA}$ ) <sup>a</sup>	0.290	0.365	0.261
$V_\tau$ ( $\text{cm}^{-1}/\text{\AA}$ )	4395	3734	2920
$K_\tau$ ( $\text{cm}^{-1}/\text{\AA}^2$ )	15155	9518	11188
$\hbar\omega_\tau$ ( $\text{cm}^{-1}$ )	70	52	57
$\Delta E_{FC}^m$ ( $\text{cm}^{-1}$ )	1912	1902	1143
$\Delta E_{JT}$ ( $\text{cm}^{-1}$ )	637	732	381
$\lambda =  \Delta E_{JT} /\hbar\omega_\tau$	6.36	8.13	4.42

<sup>a</sup>computed using values of  $R$  and  $\theta$ :  $2.014 \text{ \AA}$  and  $58.11^\circ$  ( $V(\text{CNPh})_6$ ),  $2.154 \text{ \AA}$  and  $58.70^\circ$  ( $\text{Nb}(\text{CNPh})_6$ ) and  $2.134 \text{ \AA}$  and  $57.56^\circ$  ( $\text{Ta}(\text{CNPh})_6$ ) along with  $Q_\tau^0 = \sqrt{6}R(\theta - 54.735)\pi/180$  (see also eq. S1),  $\hbar\omega = 5.806\sqrt{K_\tau G_\tau}$ ;  $G_\tau = 4/(M \cdot R^2)$ ;  $M = 103$ .

The availability of the Jahn-Teller parameters allows one to deduce the Jahn-Teller stabilization energy ( $\Delta E_{JT}$ ), defined as the difference of the electronic energies of the ground state for the octahedral non-distorted and the  $D_{3d}$  energy minimum:

$$\Delta E_{JT} = E_{Oh}({}^2T_{2g}) - E({}^2A_{1g}) = \left(\frac{1}{2}\right)(V_\tau^2/K_\tau) \quad (S6)$$

The Jahn-Teller stabilization energies of  $V(\text{CNPh})_6$ ,  $\text{Nb}(\text{CNPh})_6$  and  $\text{Ta}(\text{CNPh})_6$  are listed in Figure S28. Finally, using the values of the force constants, we compute the frequency  $\hbar\omega_\tau$  of the normal mode vibration ( $Q_\tau$ ) of 70, 52, and 57  $\text{cm}^{-1}$  for  $V(\text{CNPh})_6$ ,  $\text{Nb}(\text{CNPh})_6$ , and  $\text{Ta}(\text{CNPh})_6$ , respectively, of importance for the calculation of the spin-phonon coupling parameters (see below). These values agree *astonishingly* well to the values of the frequencies extracted from the best fitting parameters for the relaxation time  $\tilde{\nu}_1$ : 89(6), 59(4), and 66(2)  $\text{cm}^{-1}$  for  $V(\text{CNDipp})_6$ ,  $\text{Nb}(\text{CNDipp})_6$ , and  $\text{Ta}(\text{CNDipp})_6$ , respectively (Table S10).

### 3. Spin-phonon coupling parameters from first principles

Spin-phonon coupling parameters were derived using computational results from the previous section. We note that the calculation was performed on the free molecules without taking into account the solid effects such as phonon dispersion and the multitude of molecular and lattice modes which can also contribute to the relaxation mechanism. With 187 atoms, the resulting number of 555 local modes and an even larger number of lattice modes, calculation of phonon frequencies and corresponding spin-phonon coupling parameters is hardly possible. For this reason we chose to use the single effective mode approach put forward by I.B.Bersuker.<sup>16</sup> In this approximation, molecular and lattice vibration are projected onto a single mode, which in this case was taken to be the Jahn-Teller active vibration  $Q_\tau$  (Figure S27).

Application of an external magnetic field polarizes the  $S = 1/2$  spin in a  $M_S = -1/2$  state. Relaxation from this state can only proceed via a magnetic perturbation which mixes  $M_S = -1/2$  with the  $M_S = 1/2$  state. This perturbation is dynamic, caused by the movement of atoms involved in molecular vibrations or, alternatively, lattice vibrations in a solid. Here we consider the molecular origin of relaxation along a Jahn-Teller active normal mode and neglect lattice effects such a dipolar interactions and long-wavelength phonon modes. We therefore look for dynamical changes of the matrix element

$$\langle 1/2|H_Z|-1/2\rangle = \langle 1/2|\mu_B B_x g_x \hat{S}_x + \mu_B B_y g_y \hat{S}_y + \mu_B B_z g_z \hat{S}_z|-1/2\rangle \quad (S7)$$

In this study we account for the perturbation of the magnetic system using a Jahn-Teller active mode  $Q_\tau$  (soft mode) (Figure S27). We therefore look for the derivative of the matrix element with respect to this mode:  $(\partial\langle 1/2|H_Z|-1/2\rangle/\partial Q_\tau)_o$  taken at the equilibrium complex geometry “o”. Applying the Hellman-Feinmann theorem we obtain

$$\begin{aligned} (\partial\langle 1/2|H_Z|-1/2\rangle/\partial Q_\tau)_o &= \langle 1/2|(\partial H_Z/\partial Q_\tau)_o|-1/2\rangle = \mu_B B_x (\partial g_x/\partial Q_\tau)_o \langle 1/2|\hat{S}_x|-1/2\rangle + \\ &+ \mu_B B_y (\partial g_y/\partial Q_\tau)_o \langle 1/2|\hat{S}_y|-1/2\rangle + \mu_B B_z (\partial g_z/\partial Q_\tau)_o \langle 1/2|\hat{S}_z|-1/2\rangle \end{aligned} \quad (S8)$$

In an axial system herein, the  $z$ -axis was chosen along the  $C_3$  axis collinear with the magnetic anisotropy axis  $z$ . The third term at the right-hand side vanishes and we obtain:

$$\begin{aligned}
V &= (\partial\langle 1/2|H_Z|-1/2\rangle/\partial Q_\tau)_o \\
&= \mu_B B_x (\partial g_x/\partial Q_\tau)_o \langle 1/2|\hat{S}_x|-1/2\rangle + \mu_B B_y (\partial g_y/\partial Q_\tau)_o \langle 1/2|\hat{S}_y|-1/2\rangle \\
&= (1/2)\mu_B [B_x (\partial g_x/\partial Q_\tau)_o - iB_y (\partial g_y/\partial Q_\tau)_o]
\end{aligned} \tag{S9}$$

By symmetry,  $(\partial g_x/\partial Q_\tau)_o = (\partial g_y/\partial Q_\tau)_o = (\partial g_\perp/\partial Q_\tau)_o$ . Denoting the complex quantity  $1/2(B_x - iB_y)$  by  $B$ , we obtain Eqn. (4) in the main text.

To this end, we computed the first and second derivatives of the  $g$ -factors numerically. Assuming that magnetic relaxation is mostly affected by flipping of the spin via the transversal magnetic field, we computed numerically the first derivatives of the  $g_\perp$  factor for the three complexes (Table 3, main text). Spin-phonon coupling parameters ( $V_{\text{sp-ph}}$ ) were computed at the experimental magnetic fields of 2500 Oe (for V and Nb), and 2000 Oe (for Ta) according to Eq. S7 and are listed in Table 3 in the main text:

$$V_{\text{sp-ph}} = \mu_B \left( \frac{\partial g_\perp}{\partial Q_\tau} \right)_0 B \tag{S10}$$

Magnetic relaxation times ( $\tau$ ) were calculated for all three complexes at  $T = 6$  K, following the master equation previously published:<sup>19</sup>

$$\tau^{-1} = \frac{2\pi}{h} V_{\text{sp-ph}}^2 \frac{\Delta(2n+1)}{\Delta^2 + (\hbar\omega)^2} \tag{S11}$$

$$\Delta^2 = \frac{(\hbar\omega)^2 \exp(\hbar\omega/k_B T)}{(\exp(\hbar\omega/k_B T) - 1)^2} \tag{S12}$$

$$n = \frac{1}{\exp(\hbar\omega/k_B T) - 1} \tag{S13}$$

where  $n$  and  $\Delta$  have their usual meanings as the phonon occupation number and the Lorentzian broadening, respectively; the parameter  $\Delta$  was described as the Gaussian probability distribution of the phonon mode's fluctuation.

## Geometry Optimized Coordinates

V(CNDipp)<sub>6</sub>

187

Coordinates from ORCA-job vexphopt

	X	Y	Z
V	0.00000000213057	-0.00000000018796	-0.00000000017969
N	1.47570001141849	0.38265999257073	-2.79726999564410
N	-1.47569000763547	-0.38259999388417	2.79723999961347
N	-2.80252000816402	1.33927999085757	-0.70768999881174
N	2.80252000864574	-1.33927999078932	0.70768999726800
N	1.32683000685651	2.40327999527209	1.61629000841833
N	-1.32683000419851	-2.40327999519446	-1.61629001240183
C	0.84179999241842	0.34770999587216	-1.79596000630695
C	2.32195000831566	0.45838001112470	-3.89669000937382
C	2.57137989768806	-0.71968997745089	-4.61197000723443
C	3.46202004099619	-0.63641002448968	-5.66840998294466
C	4.08494998598758	0.54532001207291	-5.98473000899088
C	3.79764999363343	1.69304001414258	-5.29121000466024
C	2.91092005901265	1.68783991987154	-4.22489994745023
C	2.57398993666505	2.94804011266507	-3.45351010456282
C	1.22627003595836	3.49524996709655	-3.87155995296496
C	3.64485000974095	4.01929995789335	-3.56583996334380
C	1.88968009670633	-2.02200998918631	-4.22801001980440
C	0.48188995335787	-2.02936000227543	-4.80676999526654
C	2.64189998144664	-3.24863001310211	-4.69633997681563
C	-0.84180999617692	-0.34762000056563	1.79592000416931
C	-2.32199001172045	-0.45830000549752	3.89668000189853
C	-2.57136989297162	0.71965997770974	4.61200001039776
C	-3.46200004467464	0.63641002461138	5.66837998217786
C	-4.08491998597833	-0.54529000842904	5.98469001122919
C	-3.79766999630749	-1.69298001277235	5.29118999949831
C	-2.91093006234150	-1.68774992851531	4.22490994885475
C	-2.57395992933342	-2.94795010515922	3.45354010561520
C	-1.22630003606637	-3.49523996594730	3.87150995140607
C	-3.64483001087838	-4.01928996123898	3.56582996262425
C	-1.88967009559931	2.02207998872614	4.22802002005010
C	-0.48192995403373	2.02942000043627	4.80677999713103
C	-2.64190998288091	3.24857001523288	4.69633997648270
C	-1.70972999908015	0.97341001230773	-0.42908998749927
C	-4.06409999086515	1.71440996508173	-1.15313004976790
C	-5.17671996742571	1.15886010135843	-0.50899988474201
C	-6.42384000966378	1.49913995003929	-1.00397003431751
C	-6.55834999813317	2.32870001948319	-2.08943999173347
C	-5.45489999363576	2.88788001053965	-2.68133000054375
C	-4.17379002089037	2.59830992311637	-2.23609000039931
C	-2.94361000948998	3.21443014503215	-2.87151999188419
C	-2.40158999771891	4.34265994439967	-2.02062001573688
C	-3.18122999206358	3.68502995108353	-4.29592999400209
C	-5.00305004248427	0.22273996023534	0.67504990279439
C	-4.75754998146798	1.05340002175285	1.92664004032640

C	-6.19009997919604	-0.69025001246043	0.89149001674177
C	1.70972999858747	-0.97341001257193	0.42908998871712
C	4.06409998950730	-1.71440996161982	1.15313005254620
C	5.17671996661907	-1.15886010276983	0.50899988348019
C	6.42384000984053	-1.49913994922051	1.00397003463940
C	6.55834999805773	-2.32870001913377	2.08943999227468
C	5.45489999205811	-2.88788000989150	2.68133000079455
C	4.17379002739873	-2.59830993005770	2.23608999497952
C	2.94361000482882	-3.21443013705913	2.87152000106001
C	2.40158999656602	-4.34265994831931	2.02062001327279
C	3.18122999245065	-3.68502995202010	4.29592999055451
C	5.00305004370600	-0.22273996044187	-0.67504990164526
C	4.75754998102451	-1.05340002189120	-1.92664004077318
C	6.19009997882010	0.69025001292856	-0.89149001712350
C	0.86792001109598	1.58038000157315	0.89663999367104
C	1.74210996106244	3.38860999995796	2.50363001670688
C	2.60535011221155	3.01286998954129	3.54050989163709
C	2.96183996240967	3.99531998795935	4.44816003784909
C	2.47343000575391	5.27401000953835	4.34367999068992
C	1.65722000128405	5.62608000848790	3.29940998415800
C	1.26286996210686	4.69714994785583	2.34816006876989
C	0.36954007680328	5.07033010256508	1.18211991909993
C	1.17528996264970	5.22684996406400	-0.08937996675072
C	-0.46360002262028	6.31302996174750	1.44411002242266
C	3.11337990441938	1.58523004637098	3.65100009631928
C	4.27562004114243	1.40087998609627	2.68561995224361
C	3.54819000090484	1.21461997707043	5.05208998179739
C	-0.86792001576898	-1.58038000084341	-0.89663999190556
C	-1.74210995967933	-3.38860999587934	-2.50363001463858
C	-2.60535011254381	-3.01286999068582	-3.54050989106986
C	-2.96183996144423	-3.99531998711333	-4.44816003845359
C	-2.47343000737735	-5.27401001126777	-4.34367999122055
C	-1.65721999814517	-5.62608000413975	-3.29940998298807
C	-1.26286996638011	-4.69714995474196	-2.34816006756161
C	-0.36954007132137	-5.07033010392958	-1.18211992541632
C	-1.17528996444272	-5.22684996468866	0.08937996979813
C	0.46360002061485	-6.31302995979500	-1.44411002119898
C	-3.11337990446833	-1.58523004714318	-3.65100009681386
C	-4.27562004114088	-1.40087998589726	-2.68561995198771
C	-3.54819000084170	-1.21461997629375	-5.05208998166280
H	3.69869190607509	-1.53007848156871	-6.24043688491747
H	4.79734090789816	0.57626952331138	-6.80878311630284
H	4.29106888298065	2.62014116531059	-5.57164591672158
H	2.49887869471291	2.66069472621450	-2.39348010094584
H	0.42909285801863	2.75362559958199	-3.74199789205252
H	1.23890161050592	3.79542418436786	-4.92856753075913
H	0.95891777726750	4.37592644981891	-3.27290469394111
H	4.63773413050939	3.63541006100516	-3.29914301651756
H	3.41487076152797	4.85245683041994	-2.88928667398564
H	3.70316755061948	4.43634318335484	-4.57991890632524
H	1.81409724004377	-2.05085118346236	-3.13230444641861
H	-0.12175231888806	-1.20460417862788	-4.41212496565246

H	-0.03758636220001	-2.96458837548910	-4.57110125944672
H	0.51898834567319	-1.92891468518996	-5.89991141971654
H	3.68534930304260	-3.24956866881601	-4.35558197127606
H	2.64170880850575	-3.33660089893686	-5.79055471746030
H	2.15968738886810	-4.15384327988676	-4.30472850546178
H	-3.69865519151921	1.53007259432688	6.24042162217640
H	-4.79731755068749	-0.57622047216188	6.80874084603896
H	-4.29107305383387	-2.62009047326927	5.57162015014956
H	-2.49886077520523	-2.66060069847508	2.39350889551352
H	-0.42913323277709	-2.75358840733953	3.74193900970335
H	-1.23888777418675	-3.79540326043581	4.92852368737378
H	-0.95869943940494	-4.37584711960279	3.27288704080657
H	-4.63772801254280	-3.63543853573661	3.29913308100676
H	-3.41479882300031	-4.85240728184702	2.88924783694144
H	-3.70311662700608	-4.43636292100528	4.57989704853533
H	-1.81409622712533	2.05089132478865	3.13231329151100
H	0.12172590752335	1.20467110330022	4.41213929864368
H	0.03756324047097	2.96464741938291	4.57113462408734
H	-0.51903045391829	1.92896672235855	5.89992191806529
H	-3.68535507273827	3.24949383471833	4.35556613742033
H	-2.64175943964738	3.33651658400857	5.79055962018741
H	-2.15973380227446	4.15383717966597	4.30480498836737
H	-7.31503448227243	1.07717661747862	-0.54600475855368
H	-7.55233744614007	2.56206163505025	-2.47025485147857
H	-5.58845778054926	3.55470516551667	-3.52941360413193
H	-2.17489719197072	2.42702733640933	-2.90333336617680
H	-2.15709619759160	4.00456232100678	-1.00651310693327
H	-3.13615873624961	5.15562468917469	-1.93624100909856
H	-1.48568737239228	4.75887310197745	-2.46032562619059
H	-3.61271351453230	2.89416139468484	-4.92243522671752
H	-2.23112736827994	3.99247826671702	-4.75164806863583
H	-3.85172147580100	4.55377159258690	-4.33583574047022
H	-4.11249455050004	-0.39265920885276	0.48774917173897
H	-3.85078521904556	1.66163588154448	1.83501272516035
H	-4.64232713348723	0.41445528416346	2.80896357396881
H	-5.60298069296134	1.73106664549309	2.10717989208210
H	-6.44578142263106	-1.25785733966231	-0.01259391912606
H	-7.08211222987363	-0.13433612710603	1.20809745060635
H	-5.96449234108224	-1.41113573246449	1.68801633148824
H	7.31503416954744	-1.07717542996787	0.54600512131835
H	7.55233877841174	-2.56205919606980	2.47025292255975
H	5.58846390688374	-3.55470307707842	3.52941491949948
H	2.17491318450996	-2.42701138034514	2.90334305047003
H	2.15686079225066	-4.00447920894665	1.00660481504956
H	3.13622746014413	-5.15553933978424	1.93596045756811
H	1.48576966372307	-4.75891813816981	2.46051914594609
H	3.61273599709251	-2.89418875011558	4.92244454702857
H	2.23112254153706	-3.99244624901828	4.75166271291869
H	3.85167142701421	-4.55381254822857	4.33580680321058
H	4.11249469100042	0.39265941908402	-0.48774872726825
H	3.85079045062307	-1.66164340962491	-1.83500753410511
H	4.64231198206443	-0.41445513503546	-2.80896180461929



H	5.60298606083637	-1.73105726876801	-2.10718809864077
H	6.44578082753611	1.25785807908747	0.01259394750198
H	7.08211292796925	0.13433878015918	-1.20809873137317
H	5.96448650878378	1.41114020985127	-1.68801356065164
H	3.61575622496253	3.74470658285085	5.27970513863580
H	2.75482591858803	6.02142967034262	5.08507974334153
H	1.29706448118014	6.64939751885017	3.22953992684634
H	-0.32406291472534	4.22895358840605	1.03031569519322
H	1.73251172772296	4.31398246762937	-0.33130035218084
H	1.89882618804962	6.04857336139678	0.00446208659230
H	0.51965806965182	5.44900167639232	-0.94146335885104
H	-1.02672147542764	6.23770724421860	2.38298042402519
H	-1.18657438294281	6.45888869852604	0.63110781332361
H	0.15436735206338	7.21949677990357	1.49081694942444
H	2.29888060151633	0.91469780951288	3.34372868130545
H	3.97134387993246	1.57712540335564	1.64783724218818
H	4.68157704261450	0.38513850656429	2.74543387900178
H	5.08537959381155	2.10362586775215	2.92441102723252
H	2.75773747138199	1.39531891933592	5.79203296808891
H	4.44051201869678	1.77225851432583	5.36476767236700
H	3.80904111195615	0.14898742028757	5.09243507523023
H	-3.61575506061992	-3.74470587762807	-5.27970611419927
H	-2.75482638802175	-6.02143172440849	-5.08507762264117
H	-1.29705981239994	-6.64939474213346	-3.22953610174403
H	0.32405044684051	-4.22894823561449	-1.03029926874964
H	-1.73276300802679	-4.31411496473258	0.33122714170504
H	-1.89856122751238	-6.04880743357599	-0.00436845142532
H	-0.51952545502428	-5.44880636644291	0.94142909193399
H	1.02673512960263	-6.23766497744760	-2.38297400552581
H	1.18654856903331	-6.45891614529082	-0.63109132362792
H	-0.15435243789623	-7.21950144585419	-1.49089765920051
H	-2.29888058935358	-0.91469804756299	-3.34372946139434
H	-3.97134217013957	-1.57711763356108	-1.64783663512645
H	-4.68158382599945	-0.38514184185497	-2.74544223528423
H	-5.08537484938912	-2.10363342359165	-2.92440528560191
H	-2.75774157844798	-1.39533519855174	-5.79203386289117
H	-4.44052492726160	-1.77223794797145	-5.36476428513951
H	-3.80900372150121	-0.14897543951808	-5.09243876667574

Nb(CNDipp)<sub>6</sub>

187

Coordinates from ORCA-job nbexphopt

	X	Y	Z
Nb	-0.00000000559356	-0.00000000329551	-0.00000000042884
C	1.39919005367011	-0.66023000112049	1.49896995030170
N	2.21188997475434	-0.78714000192901	2.35546002774369
C	3.19595999599566	-0.89589000882471	3.32963999775077
C	2.94525994010630	-0.32412999558984	4.58346002865421
C	3.96991001065156	-0.38646000408446	5.51473997819420
C	5.17231001458626	-0.97998998612807	5.22093000139373
C	5.37638997855918	-1.56481002277656	3.99769000833125
C	4.40205001228985	-1.53787991902130	3.01006000256395
C	4.60894004064280	-2.17724013995452	1.64957000023705
C	3.90766999712071	-3.52128994557274	1.56429999461725
C	6.07912996748453	-2.31250994846572	1.28079000020676
C	1.62336004752774	0.35880995398211	4.88399999071010
C	0.57511999161848	-0.69178999048878	5.22644999541973
C	1.71177997455354	1.38306003721747	6.00007000414518
C	-1.39920004208961	0.66023000565385	-1.49899996040592
N	-2.21195998750434	0.78721999194091	-2.35545001664287
C	-3.19603999043402	0.89592001814714	-3.32958000720697
C	-2.94525993735198	0.32411000129669	-4.58343002615970
C	-3.96985000863256	0.38637000335309	-5.51473997620279
C	-5.17231001428096	0.97998999025601	-5.22093000384831
C	-5.37635997811739	1.56479002489112	-3.99766001484464
C	-4.40202002517045	1.53791990704770	-3.01011996790144
C	-4.60893001364507	2.17732015524893	-1.64953003399561
C	-3.90767000408039	3.52117993524080	-1.56424998013539
C	-6.07909998172454	2.31249994747995	-1.28078999347591
C	-1.62340004993904	-0.35878995727870	-4.88400999155913
C	-0.57511999103590	0.69176999331652	-5.22640999501790
C	-1.71175997513592	-1.38310003919050	-6.00001000566632
C	-0.93396998834994	-1.92246000884326	-0.26931996143324
N	-1.61030000809801	-2.89848999889644	-0.25751003597189
C	-2.40312999930490	-4.03659998827030	-0.18505999087359
C	-3.74393000811570	-3.92924997751335	-0.57575004209010
C	-4.53014998810156	-5.06115999762751	-0.42868998128995
C	-4.01813000220350	-6.23059001640567	0.07616999134266
C	-2.69251999992005	-6.31766997858080	0.41555998805932
C	-1.84278004395654	-5.22645996390015	0.30395008253642
C	-0.37352990843790	-5.30167014722032	0.67594984890572
C	0.49766996761858	-5.43635994597464	-0.56023992447590
C	-0.07480002784890	-6.41489993692196	1.66949003943019
C	-4.30558996659272	-2.62056004302925	-1.10099002922999
C	-3.93309000579074	-2.46065999381412	-2.56914998175429
C	-5.80856002021183	-2.49660996968430	-0.93316999272814
C	0.93396998919306	1.92246000775269	0.26931996148925
N	1.61030000840117	2.89848999558233	0.25751003772001
C	2.40312999537797	4.03660000100981	0.18505999553108
C	3.74393000750305	3.92924997317645	0.57575004032034

C	4.53014998849858	5.06115999869176	0.42868998213385
C	4.01813000143043	6.23059001269871	-0.07616999536635
C	2.69251999793519	6.31766998736770	-0.41555998364660
C	1.84278005931727	5.22645994547759	-0.30395008262596
C	0.37352989444584	5.30167016321337	-0.67594986088873
C	-0.49766996279181	5.43635994567536	0.56023992555307
C	0.07480003190052	6.41489992793118	-1.66949003444980
C	4.30558996719615	2.62056004586557	1.10099002908940
C	3.93309000526867	2.46065999322748	2.56914998179159
C	5.80856002067845	2.49660996898478	0.93316999280918
C	1.36351998490932	-0.20095004872674	-1.65563001023142
N	1.94487000911521	-0.19047996627230	-2.69107000112481
C	2.57476999614531	-0.19337000591091	-3.92906000748290
C	2.90866006259515	1.04164005571227	-4.49913994387945
C	3.47336997103963	1.01339997593381	-5.76455999836212
C	3.69395000166994	-0.16898000115774	-6.42632001606052
C	3.39155002882264	-1.36519999207175	-5.82827998428718
C	2.81728987411465	-1.41970996807507	-4.56622002911179
C	2.47345022356551	-2.73290009256554	-3.88809996313478
C	3.51754989812460	-3.10207997131341	-2.84955002826520
C	2.27239993292637	-3.87096995889008	-4.87806999886103
C	2.62854001835104	2.34343994025428	-3.77052002423031
C	3.72351998924991	2.59601000424619	-2.74240000028314
C	2.50305997351609	3.53962004217089	-4.69577999378724
C	-1.36351997466358	0.20095006276454	1.65563001717889
N	-1.94487002393975	0.19047996003104	2.69106999566422
C	-2.57476997242931	0.19336999816446	3.92906000396832
C	-2.90866006175446	-1.04164005309365	4.49913994923148
C	-3.47336997282719	-1.01339997629717	5.76455999674804
C	-3.69395000376810	0.16898000093187	6.42632001864212
C	-3.39155001447899	1.36519999041330	5.82827997636148
C	-2.81728991944277	1.41970997386091	4.56622003843597
C	-2.47345018317945	2.73290009566999	3.88809996908780
C	-3.51754991759524	3.10207997051939	2.84955002000790
C	-2.27239994038954	3.87096995604510	4.87806999552172
C	-2.62854001870664	-2.34343994175935	3.77052002124520
C	-3.72351998905373	-2.59601000420542	2.74240000109559
C	-2.50305997468122	-3.53962004052307	4.69577999467215
H	3.82797099669602	0.06506384309390	6.49358329802375
H	5.96329079674177	-1.00060956025981	5.96998400039795
H	6.33124746828897	-2.04170016695576	3.79066598048073
H	4.13798537237547	-1.51304089376282	0.90917748591230
H	2.83579182990351	-3.43138178498005	1.77784357801512
H	4.33732248936175	-4.23150600916496	2.28407914571174
H	4.00990578660324	-3.95142131954753	0.55888653453487
H	6.61177917579545	-1.35755934447370	1.37311711793804
H	6.17711647105896	-2.65241608235871	0.24176275662647
H	6.59370861749529	-3.05039384838815	1.91017602280070
H	1.30192439795730	0.87376354221680	3.96769139085802
H	0.41034714254487	-1.38655505451426	4.39476024935103
H	-0.38751847319739	-0.22523635236153	5.46376817426255
H	0.89121340140742	-1.27859858448999	6.09969962629047

H	2.49263472886296	2.13153635115470	5.81333016217279
H	1.91453049824217	0.91407838776811	6.97178910774083
H	0.75436713337341	1.91148462513885	6.09486816675751
H	-3.82790629048444	-0.06515983967852	-6.49357684102205
H	-5.96329423014137	1.00060054283488	-5.96997844906659
H	-6.33121556220348	2.04169140909725	-3.79064661666346
H	-4.13799154864705	1.51301847868696	-0.90921270323519
H	-2.83570685594455	3.43119473277207	-1.77725762492542
H	-4.33686209151131	4.23132555245380	-2.28439780932191
H	-4.01044084410618	3.95140459007808	-0.55887128359939
H	-6.61172373310746	1.35755612773678	-1.37323023778920
H	-6.17715105401466	2.65228668274381	-0.24172614624583
H	-6.59364175013348	3.05047862982941	-1.91009670071669
H	-1.30195143510901	-0.87373366291547	-3.96769319112865
H	-0.41036040324287	1.38652692496184	-4.39471088876476
H	0.38751298214276	0.22518531018872	-5.46368548725606
H	-0.89114869357390	1.27859640396426	-6.09967286492406
H	-2.49260326706332	-2.13158305778556	-5.81324836431817
H	-1.91448618446958	-0.91419545257304	-6.97177277737749
H	-0.75433109197572	-1.91151037534144	-6.09473290832155
H	-5.58265954688616	-5.01693696060067	-0.69803582830853
H	-4.66539282607686	-7.09933259699086	0.19225309255589
H	-2.30465542337224	-7.25737494910415	0.80103570466399
H	-0.11612470335780	-4.34574481734030	1.15675562843617
H	0.32837558149648	-4.61312885482499	-1.26463203690709
H	0.28815346081850	-6.37874953386813	-1.08494004221261
H	1.56215506272159	-5.42704668058213	-0.28963155486251
H	-0.71772159422162	-6.35389885937509	2.55670093632365
H	0.96795799015134	-6.34896872263681	2.00565619519606
H	-0.20553926582796	-7.40912110881204	1.22258608333369
H	-3.82878510979453	-1.80665001564229	-0.53666141421998
H	-2.84647000357113	-2.44785151770903	-2.71171726783114
H	-4.33197514651250	-1.52583885608778	-2.97825147374673
H	-4.34301761252234	-3.29156163872138	-3.15932586244771
H	-6.12253366603760	-2.66804305586184	0.10451913016016
H	-6.35290394777159	-3.20148957632819	-1.57519492709448
H	-6.13223114978149	-1.48768698654717	-1.22009940997813
H	5.58265891412277	5.01693815845879	0.69803869704997
H	4.66539063404612	7.09933393831109	-0.19225471647629
H	2.30464783088934	7.25737097577383	-0.80103830909599
H	0.11610894164631	4.34576392776008	-1.15678202790860
H	-0.32809522745709	4.61342459505648	1.26492191432965
H	-0.28854461821418	6.37902964434377	1.08457159142884
H	-1.56211598642097	5.42667086454431	0.28952723186527
H	0.71768323125903	6.35380587187557	-2.55673402044820
H	-0.96798373231030	6.34902337724924	-2.00557803203415
H	0.20568022083865	7.40914329622466	-1.22267454876147
H	3.82878591725488	1.80665057976648	0.53666019055068
H	2.84647009406487	2.44784917547574	2.71171641322313
H	4.33197914492308	1.52584037966003	2.97825083183113
H	4.34301469300969	3.29156416283208	3.15932431188906
H	6.12253363934994	2.66805969376870	-0.10451671102524

H	6.35290908720110	3.20147233225092	1.57520837718206
H	6.13222483548382	1.48767233979014	1.22006904697823
H	3.72704760619434	1.94964612816433	-6.25581018440893
H	4.12639728983961	-0.15724338576192	-7.42630522280173
H	3.58713214593510	-2.29001186423483	-6.36538531727153
H	1.52154128743957	-2.57881093870866	-3.35761938094704
H	3.63829945623704	-2.31247552308629	-2.09807047613002
H	4.49468269578090	-3.27234111471849	-3.32227461254089
H	3.23134951676064	-4.02096120335831	-2.32000408579846
H	1.54638427422162	-3.60903780535149	-5.65795887224698
H	1.89837625597528	-4.76119937710435	-4.35617095284349
H	3.21116127387602	-4.15784525054554	-5.36971824479975
H	1.67756958835720	2.22149549309173	-3.23296613625529
H	3.77416170127649	1.79051236149994	-2.00095519109907
H	3.54998130638817	3.53328119626800	-2.20216749874395
H	4.70282873621695	2.66526597494363	-3.23529043011058
H	1.76336338301593	3.37305765832916	-5.48946671662590
H	3.46033092131194	3.79322461121787	-5.16965943644840
H	2.18780865050829	4.42046047728595	-4.12160230719790
H	-3.72704454049180	-1.94964590116668	6.25581185312775
H	-4.12639985164000	0.15724505444846	7.42630419644850
H	-3.58712951733467	2.29001438896651	6.36538132283670
H	-1.52154902901777	2.57880377298958	3.35760890907434
H	-3.63835429100025	2.31234240840513	2.09820929578594
H	-4.49466322632844	3.27241300466296	3.32228595514864
H	-3.23152719552421	4.02075045916283	2.31962054916050
H	-1.54635626603044	3.60906332689747	5.65794161331635
H	-1.89841113949555	4.76120942731519	4.35616220046462
H	-3.21115545503203	4.15782143841107	5.36974129557051
H	-1.67756978788259	-2.22149625673438	3.23296526012192
H	-3.77416418344062	-1.79051013225318	2.00095777630175
H	-3.54998008683699	-3.53327905132244	2.20216413289186
H	-4.70282834615494	-2.66526930870675	3.23529092064924
H	-1.76333454234731	-3.37307770499603	5.48944326701684
H	-3.46032523214701	-3.79318995201993	5.16969191430304
H	-2.18787882786543	-4.42047295997068	4.12159592210435

Ta(CNDipp)<sub>6</sub>

187

Coordinates from ORCA-job taexphopt

	X	Y	Z
Ta	-0.00000001352551	-0.00000000456145	-0.00000000255063
N	0.11464196829109	-2.82816598325751	-1.72352602145491
N	2.39271101013056	1.51203300078379	-1.72352600647094
N	-2.50504498395090	1.31479899788865	-1.72352601190135
N	-0.11302698197416	2.82723198980679	1.72147801797124
N	-2.39109601136546	-1.51296599894952	1.72147800559590
N	2.50665996826205	-1.31573301128382	1.72147803513220
C	0.07224701863040	-1.80108700704150	-1.14618998361512
C	-0.13041506010740	-4.11164796602919	-2.18211908274006
C	0.82403801211076	-4.70774502607453	-3.02209298070241
C	0.58144299706092	-6.01761399781587	-3.43271999743690
C	-0.55997698617590	-6.68780700197580	-3.02443198601248
C	-1.48980906068989	-6.07251897337294	-2.20083707683122
C	-1.30099582886345	-4.76411706405082	-1.75569780742508
C	-2.28822613360877	-4.04061698184169	-0.85956913672877
C	-3.20705497701190	-4.98360499766856	-0.09446796844049
C	-3.11549495862309	-3.02273300450324	-1.65713496194305
C	2.04247500794010	-3.91881197812035	-3.45348599012000
C	1.65346199669445	-2.91265600595279	-4.54147399961519
C	3.20713100237299	-4.79263500506581	-3.91939100365829
C	1.52443200218636	0.96177799612191	-1.14619000246977
C	3.62676796630518	1.94154804368800	-2.18211895403895
C	3.66577700182018	3.06617698164826	-3.02209300975968
C	4.92145399906847	3.51101800860348	-3.43271999083596
C	6.07256800886136	2.85761599268417	-3.02443201377698
C	6.00462897521036	1.74471402581635	-2.20083696737626
C	4.77711206945888	1.25402992554070	-1.75569807518813
C	4.64415793452438	0.03731404380411	-0.85956894818003
C	5.92022501906908	-0.28692100750803	-0.09446801271082
C	4.17628000717288	-1.18806401808382	-1.65713501182129
C	2.37332200827352	3.72690900666957	-3.45348600906133
C	1.69647199520034	2.88693500181887	-4.54147399570880
C	2.54774699821845	5.17244199646568	-3.91939099586379
C	-1.59437199364022	0.83797400781947	-1.14619000468077
C	-3.49404509648846	2.16876597987058	-2.18211888646211
C	-4.48750697363566	1.64023400115049	-3.02209302513010
C	-5.50058900309201	2.50526200154995	-3.43272000067724
C	-5.51028398899380	3.82885700399838	-3.02443200806893
C	-4.51251306527618	4.32647098670082	-2.20083693457214
C	-3.47380983802360	3.50875305416936	-1.75569818441450
C	-2.35362609678969	4.00196894073384	-0.85956887055675
C	-2.71086298644896	5.26919300838162	-0.09446803003254
C	-1.05847798298316	4.20946402729920	-1.65713504035628
C	-4.41349000135657	0.19057000736492	-3.45348600251517
C	-3.34762600029554	0.02438699801869	-4.54147399790791
C	-5.75257100195121	-0.38114000190772	-3.91939099728268
C	-0.07063201504147	1.80015301021673	1.14414298807990

C	0.13203006199920	4.11071396069755	2.18007108458530
C	-0.82242301331850	4.70681202131011	3.02004498389899
C	-0.57982799647260	6.01668000038782	3.43067300166834
C	0.56159198763668	6.68687399923500	3.02238498602053
C	1.49142406148982	6.07158597483645	2.19878907629857
C	1.30261083090123	4.76318306886669	1.75364980578923
C	2.28984113473465	4.03968298231479	0.85752213732176
C	3.20866997300017	4.98267200051207	0.09241996761498
C	3.11710995978841	3.02180000146829	1.65508796114624
C	-2.04086000672185	3.91787898128358	3.45143798963913
C	-1.65184700080645	2.91172200801771	4.53942699929251
C	-3.20551600122417	4.79170200731223	3.91734300295653
C	-1.52281699160059	-0.96271199798945	1.14414300608326
C	-3.62515296586176	-1.94248203726852	2.18007095964408
C	-3.66416200051221	-3.06711097950032	3.02004500925629
C	-4.91983899801476	-3.51195201176799	3.43067299568149
C	-6.07095300721178	-2.85854999098272	3.02238501281598
C	-6.00301397485108	-1.74564802541063	2.19878897092364
C	-4.77549706554381	-1.25496393868648	1.75365006365268
C	-4.64254293708936	-0.03824803975588	0.85752195555509
C	-5.91861001675959	0.28598800869302	0.09242001051157
C	-4.17466500526028	1.18713101818097	1.65508800950154
C	-2.37170700673063	-3.72784200432622	3.45143800828034
C	-1.69485699939758	-2.88786899954710	4.53942699545822
C	-2.54613199706596	-5.17337599956556	3.91734299547618
C	1.59598700379997	-0.83890799962972	1.14414299767011
C	3.49566010601068	-2.16969997142263	2.18007087593970
C	4.48912197732843	-1.64116799864381	3.02004502185581
C	5.50220399849546	-2.50619600448126	3.43067300585197
C	5.51189899025850	-3.82979100218207	3.02238500805313
C	4.51412806197184	-4.32740498318093	2.19878893264898
C	3.47542483552185	-3.50968606129992	1.75365018941096
C	2.35524110015019	-4.00290293504151	0.85752186666136
C	2.71247798216137	-5.27012700702011	0.09242003044255
C	1.06009298338684	-4.21039802583399	1.65508804094970
C	4.41510500209605	-0.19150300476675	3.45143800207260
C	3.34924100158843	-0.02532100108376	4.53942699758175
C	5.75418599794279	0.38020699892273	3.91734299695681
H	1.29776184172451	-6.52334706787230	-4.07536866517627
H	-0.72898052916702	-7.71272968700628	-3.35341002259839
H	-2.37529235664396	-6.62276099525237	-1.89259878796477
H	-1.70646134744033	-3.46111746733269	-0.13002903458034
H	-2.64162681430992	-5.73263112013918	0.47512545958095
H	-3.89396137436589	-5.51647617475961	-0.76575665447635
H	-3.82144911918838	-4.41687430270241	0.61390731978614
H	-2.49359958063709	-2.18800863048502	-1.99910057321713
H	-3.89669227257526	-2.59365966713955	-1.01550181159565
H	-3.60131561904222	-3.49041833504362	-2.52312500569852
H	2.38242931409578	-3.34794573440030	-2.57814571524559
H	0.86126537645203	-2.24064245329253	-4.19163768665827
H	1.29321269603506	-3.43352384174640	-5.43855692140675
H	2.51474962154226	-2.29319509671866	-4.82515411667178

H	3.47490402471282	-5.54637919021368	-3.16846627713109
H	4.09119642873891	-4.16843856577247	-4.10099190942269
H	2.97840335318719	-5.31295202342612	-4.85894920415557
H	5.00147368033584	4.38492926438136	-4.07445736088853
H	7.04491563842347	3.22424201756686	-3.35205905746512
H	6.92386687986489	1.25343461958159	-1.89166261809225
H	3.85282756233048	0.25407917527920	-0.12917587238495
H	6.29005657696236	0.57948703787552	0.46917743860366
H	6.72349048189064	-0.62176039256463	-0.76453423653838
H	5.73261770156379	-1.09704056556393	0.61881570375499
H	3.12877779699377	-1.08458088519554	-1.96184353755893
H	4.23557745408093	-2.08643811056765	-1.02805726636820
H	4.79949766594223	-1.35006358600057	-2.54581926919906
H	1.70823888735880	3.73604302640614	-2.57871101931478
H	1.51020097914894	1.86603712537353	-4.18886689416909
H	2.32754594517343	2.83322865951055	-5.43848850269159
H	0.72964887637642	3.32395701324431	-4.82483975010274
H	3.06029455025773	5.78336156511857	-3.16578141428623
H	1.56567933938260	5.62373894464220	-4.10895789370782
H	3.11923824168955	5.23390552018670	-4.85504301717944
H	-6.29661867190371	2.13760287991285	-4.07540320878802
H	-6.31350053771613	4.48773432785008	-3.35297783675247
H	-4.54563608916554	5.36837869993353	-1.89240872075757
H	-2.14404164488244	3.20886755061451	-0.12925992234748
H	-3.64674093072215	5.15538845997659	0.46793245199170
H	-2.82106725518742	6.13323255050323	-0.76349981264746
H	-1.91638082828746	5.51063585094498	0.62030021700652
H	-0.61991079768476	3.24871306907170	-1.95001038294839
H	-0.31330009746782	4.71848550196433	-1.03114476976655
H	-1.22941469442973	4.82137618358761	-2.55192704153467
H	-4.08846074519733	-0.38820048875093	-2.57775226936392
H	-2.36958505452324	0.37104121747760	-4.18817717550696
H	-3.61502010553056	0.60012132635398	-5.43751193394137
H	-3.24495452763463	-1.03088075650844	-4.82764333389934
H	-6.54020348544096	-0.23689372148530	-3.16938909011905
H	-5.65410925204283	-1.45861016172915	-4.10237613436734
H	-6.08693157722662	0.07878243142393	-4.85879176637444
H	-1.29614431730163	6.52241685209429	4.07332461891626
H	0.73059741411162	7.71179712363366	3.35136456637100
H	2.37690644115159	6.62184329758296	1.89056364226605
H	1.70785329406249	3.46034366309963	0.12803751917054
H	2.64325633061218	5.73175203223104	-0.47711842294966
H	3.89561308229157	5.51548725138143	0.76371569991362
H	3.82303437279426	4.41595066695544	-0.61599015855440
H	2.49527106038023	2.18657945763456	1.99597795487610
H	3.89900280606902	2.5934777607039	1.01378460577746
H	3.60202672281822	3.48919514244192	2.52173305394832
H	-2.38078851432028	3.34699107900357	2.57610432326967
H	-0.85941246545160	2.23996607340662	4.18962979581922
H	-1.29187750899012	3.43259473891460	5.43662141278745
H	-2.51303090994109	2.29201324624463	4.82287803534530
H	-3.47330839639798	5.54543237274284	3.16640983695208



H	-4.08957609774777	4.16750380457186	4.09897177889147
H	-2.97677576704717	5.31203966496701	4.85688799461580
H	-4.99986812634992	-4.38585875099176	4.07241869039028
H	-7.04330032191153	-3.22517113477357	3.35002265778773
H	-6.92225758030356	-1.25436991675146	1.88962262852400
H	-3.85119754854682	-0.25510320829350	0.12718363506968
H	-6.28842572613471	-0.58040523760692	-0.47126162306736
H	-6.72188315331031	0.62078161059330	0.76249891814202
H	-5.73102109299579	1.09614406540624	-0.62082879888427
H	-3.12747197444971	1.08316975052276	1.96065094719226
H	-4.23303103382568	2.08536330393210	1.02572383657957
H	-4.79851265603896	1.34963553450618	2.54324339456366
H	-1.70661901776827	-3.73696308535828	2.57666792107855
H	-1.50854141284859	-1.86702239584851	4.18669371503886
H	-2.32596645642518	-2.83406585980721	5.43640888474363
H	-0.72805757002515	-3.32491129938499	4.82285021828929
H	-3.05868315800005	-5.78430069486957	3.16373781804860
H	-1.56406724541083	-5.62467925593730	4.10692281201885
H	-3.11763131865097	-5.23483885091842	4.85299071504801
H	6.29822819857861	-2.13853644011585	4.07336142594150
H	6.31510875904030	-4.48867180655439	3.35093927857603
H	4.54724771094308	-5.36931538030167	1.89036963721657
H	2.14575688925581	-3.20971614450503	0.12728020338298
H	3.64837621860223	-5.15635723062728	-0.46995488244890
H	2.82263510588703	-6.13416107200941	0.76146422695927
H	1.91800248577923	-5.51155937801781	-0.62235878366852
H	0.62118531462985	-3.24962633574481	1.94740436161088
H	0.31509564193272	-4.71991577596960	1.02928373391870
H	1.23110940019459	-4.82182043184107	2.55019331455034
H	4.09006669613212	0.38727799890047	2.57571325971391
H	2.37121468375562	-0.37212052786854	4.18623662272469
H	3.61673618821048	-0.60091722676142	5.43552445325248
H	3.24646178767288	1.02996897948436	4.82546964940967
H	6.54182224896717	0.23597018080104	3.16734230252918
H	5.65571731932567	1.45767487727643	4.10033437902070
H	6.08854702296069	-0.07971799482612	4.85674175545521

DFT optimized geometries for the M(CNPh)<sub>6</sub> truncated model complexes for CASSCF/NEVPT2 calculations.

V(CNNp)<sub>6</sub>

79

Coordinates from ORCA-job vtruncopt

V	0.00000000975195	-0.00000000454446	-0.00000000023898
N	1.47569995601907	0.38266005398776	-2.79727002542825
N	-1.47568995562540	-0.38260005626666	2.79724002567755
N	-2.80251997359811	1.33928008053492	-0.70768998940042
N	2.80251997358564	-1.33928007991006	0.70768999044522
N	1.32683002679113	2.40328004478296	1.61628992727499
N	-1.32683003803729	-2.40328004102116	-1.61628992789690
C	0.84180010586886	0.34771002295979	-1.79595993574276
C	2.32194995283787	0.45837995954436	-3.89669001784350
C	2.57137998603226	-0.71968998785714	-4.61197002276927
C	3.46201998269261	-0.63640999723333	-5.66841001464226
H	3.64355001809386	-1.41144000319453	-6.18676998502144
C	4.08495003078335	0.54531998602611	-5.98472997356084
H	4.72093996506035	0.56838000942370	-6.68936002682299
C	3.79765014616461	1.69303998662873	-5.29120986900098
H	4.21554991608556	2.50762001381186	-5.54474006827575
C	2.91091998132494	1.68783999258341	-4.22490003306676
C	-0.84181010687869	-0.34762002514987	1.79591993577797
C	-2.32198995276034	-0.45829995875237	3.89668001670565
C	-2.57136998441045	0.71965998869973	4.61200002204452
C	-3.46199998578644	0.63640999745076	5.66838001503420
H	-3.64354001628541	1.41136000737508	6.18678998820737
C	-4.08492003201649	-0.54528998153411	5.98468997279379
H	-4.72098996670737	-0.56846001052325	6.68933002802290
C	-3.79767014954659	-1.69297998860894	5.29118986564403
H	-4.21553991969795	-2.50761001235879	5.54471006942749
C	-2.91092998262492	-1.68774999006259	4.22491003478702
C	-1.70972998975471	0.97340994080177	-0.42909012600805
C	-4.06410000387013	1.71440999570924	-1.15312992695984
C	-5.17672000461018	1.15886003182581	-0.50899998571203
C	-6.42384000473628	1.49914001171531	-1.00396999245238
H	-7.20218999726008	1.15451998897577	-0.58249001124387
C	-6.55834999843521	2.32869995593664	-2.08944002336405
H	-7.42287999961115	2.51664003996311	-2.43417996935884
C	-5.45489997177325	2.88787985778261	-2.68133014847927
H	-5.56978001273135	3.48405008442140	-3.41201991957383
C	-4.17379002295592	2.59831002238500	-2.23608996711685
C	1.70972998942245	-0.97340994080741	0.42909012454871
C	4.06410000381514	-1.71440999605015	1.15312992699858
C	5.17672000456467	-1.15886003185987	0.50899998567938
C	6.42384000470183	-1.49914001125159	1.00396999281213
H	7.20218999726513	-1.15451998923210	0.58249001104713
C	6.55834999843003	-2.32869995595989	2.08944002336709
H	7.42287999961343	-2.51664004000107	2.43417996932781
C	5.45489997183871	-2.88787985793807	2.68133014825987

H	5.56978001270937	-3.48405008429122	3.41201991970565
C	4.17379002287315	-2.59831002243676	2.23608996713830
C	0.86791986819792	1.58038002458543	0.89664006209954
C	1.74211007003455	3.38860995070725	2.50362998809764
C	2.60535002439545	3.01287002041498	3.54050997914980
C	2.96183999251219	3.99531999821506	4.44816000939425
H	3.55865000047839	3.78157999695539	5.15552000242506
C	2.47342995883233	5.27400998072233	4.34368003110824
H	2.70199004450090	5.92054001082671	5.00058997086046
C	1.65721981679074	5.62607997076241	3.29941009134118
H	1.35423009275310	6.52355001939573	3.22679994489437
C	1.26287004644269	4.69715000890695	2.34815999446578
C	-0.86791988007765	-1.58038002252159	-0.89664005661098
C	-1.74211005808736	-3.38860995499175	-2.50362998847462
C	-2.60535006050836	-3.01287002859873	-3.54050995679225
C	-2.96184001409689	-3.99532000582453	-4.44815999245550
H	-3.55864999759849	-3.78157999623812	-5.15552000471123
C	-2.47342995694871	-5.27400997997933	-4.34368003316194
H	-2.70199003635360	-5.92054000851856	-5.00058997657070
C	-1.65721982375303	-5.62607997275711	-3.29941008622979
H	-1.35423008917548	-6.52355001834604	-3.22679994737381
C	-1.26287003308294	-4.69715000394483	-2.34816000557325
H	-2.97612716945826	-2.00228877719798	-3.62797361681898
H	-0.60487046213486	-4.94261320496115	-1.51918577639767
H	-3.28065207288059	3.01348285307388	-2.69484291473790
H	-5.03777092384894	0.49361933596975	0.33873870215462
H	-2.67554538067985	-2.57756228686921	3.64760883239001
H	-2.07384321944985	1.64309504621568	4.32861744489422
H	2.96261944202403	1.98888385831844	3.60612629193048
H	0.60488923268040	4.94304253228090	1.51925276298895
H	2.07386761759494	-1.64311707684579	-4.32854515064092
H	2.67553988580956	2.57765892668242	-3.64760953198565
H	5.03777483315004	-0.49362698035482	-0.33874600795176
H	3.28065471665711	-3.01349096292002	2.69484201037266

Nb(CNPh)<sub>6</sub>

79

Coordinates from ORCA-job nbtruncopt

Nb	-0.00000001578302	0.00000000188845	0.00000001534536
C	1.39919008411340	-0.66023010879996	1.49896990329128
N	2.21189003539753	-0.78713980182146	2.35545999606052
C	3.19595991949484	-0.89589011292341	3.32964005105896
C	2.94525999813270	-0.32413002234171	4.58346000927822
C	3.96991002664986	-0.38645991511732	5.51473997510867
H	3.83742998900071	-0.01027003763858	6.37700001343763
C	5.17231000509998	-0.97998998661744	5.22092999082848
H	5.86680999057774	-0.98307002345116	5.86847001237468
C	5.37639002169070	-1.56480995909225	3.99768998078073
H	6.20380999407854	-1.99919001537891	3.82321000584967
C	4.40204999242705	-1.53788002673726	3.01006001302597
C	-1.39920006120841	0.66023006709485	-1.49899993173729
N	-2.21196002147689	0.78721988491504	-2.35544999653002
C	-3.19603994547140	0.89592006295343	-3.32958003623804
C	-2.94526000197577	0.32411001590223	-4.58343000039432
C	-3.96985002291783	0.38636991739733	-5.51473997463982
H	-3.837444998533914	0.01021003804105	-6.37699001336797
C	-5.17231000597215	0.97998998783124	-5.22092999073472
H	-5.86673999487429	0.98302001187432	-5.86854000811150
C	-5.37636000206591	1.56479000337608	-3.99766000250377
H	-6.20378999961476	1.99919999909540	-3.82324999812214
C	-4.40201998917158	1.53792004002582	-3.01012001345150
C	-0.93396986717067	-1.92246009066553	-0.26931996801145
N	-1.61030010854380	-2.89848991978318	-0.25750985573358
C	-2.40312997511545	-4.03660001315712	-0.18506014268453
C	-3.74392999051014	-3.92925001295159	-0.57575001683498
C	-4.53015002983970	-5.06115996815484	-0.42868992396011
H	-5.44471999063730	-5.02791001500947	-0.68357003285693
C	-4.01813000085559	-6.23058999434240	0.07617001336417
H	-4.58670999642269	-6.98212000580075	0.19281997325447
C	-2.69252000746844	-6.31766998658073	0.41556004710641
H	-2.34828999516852	-7.14485000556379	0.73342998293895
C	-1.84277999710641	-5.22646000984070	0.30394997440267
C	0.93396986770935	1.92246009062598	0.26931996863229
N	1.61030010829496	2.89848992009561	0.25750985498970
C	2.40312997508093	4.03660001323922	0.18506014273477
C	3.74392999050634	3.92925001291634	0.57575001681894
C	4.53015002983137	5.06115996815922	0.42868992396632
H	5.44471999063925	5.02791001501619	0.68357003286704
C	4.01813000084892	6.23058999435018	-0.07617001331742
H	4.58670999642742	6.98212000579277	-0.19281997328811
C	2.69252000746934	6.31766998657403	-0.41556004707323
H	2.34828999515968	7.14485000556150	-0.73342998292792
C	1.84277999710984	5.22646000982354	-0.30394997445055
C	1.36352002118468	-0.20095015984687	-1.65562999100038
N	1.94486984591743	-0.19047991740028	-2.69107008752821
C	2.57477012235927	-0.19336998025332	-3.92905992731719

C	2.90866002283064	1.04163999282603	-4.49913999706278
C	3.47336992030869	1.01340001137398	-5.76456003184188
H	3.71427003572950	1.83095999397685	-6.18417998334707
C	3.69394998644954	-0.16897999988265	-6.42632000455113
H	4.05585002363914	-0.15706999889806	-7.30402998786372
C	3.39154995672169	-1.36520000418520	-5.82828001881147
H	3.58079001464309	-2.17509999729542	-6.28872999257639
C	2.81729002574495	-1.41971000155465	-4.56621999207427
C	-1.36352002123286	0.20095015979845	1.65562999093490
N	-1.94486984561038	0.19047991791319	2.69107008747765
C	-2.57477012227769	0.19336998017985	3.92905992725461
C	-2.90866002276320	-1.04163999283790	4.49913999706592
C	-3.47336992035150	-1.01340001138292	5.76456003183046
H	-3.71427003572949	-1.83095999397526	6.18417998336586
C	-3.69394998647501	0.16897999988064	6.42632000454771
H	-4.05585002360756	0.15706999890277	7.30402998787934
C	-3.39154995683178	1.36520000415672	5.82828001876853
H	-3.58079001462021	2.17509999730473	6.28872999257915
C	-2.81729002570330	1.41971000155336	4.56621999208864
H	-4.56408189442099	1.98930909652608	-2.04245072227020
H	-1.98872866429868	-0.14982668686282	-4.78503242848863
H	-4.12588090833036	-2.98819798941441	-0.96143990250865
H	-0.79314057926185	-5.26254114094322	0.58195256171086
H	2.71287772040871	1.96302287727724	-3.95786702350890
H	2.55188853032445	-2.35232913226303	-4.07629455168712
H	0.79313990281174	5.26253974260104	-0.58194966316956
H	4.12588013405719	2.98820104665401	0.96144709016902
H	-2.71287439364051	-1.96302328676796	3.95786923744763
H	-2.55188704314750	2.35232796829256	4.07629370748887
H	4.54352176585871	-1.97761443816855	2.02678380710481
H	1.98879862708386	0.14979999343246	4.78557477289882

Ta(CNPh)<sub>6</sub>

79

Coordinates from ORCA-job tatruncopt

Ta	-0.00000000147790	-0.00000003778458	0.00000001362142
N	0.11464211054251	-2.82816607162414	-1.72352587207564
N	2.39271100880839	1.51203313313367	-1.72352587566939
N	-2.50504505706285	1.31479896696542	-1.72352593689549
N	-0.11302710126711	2.82723206696772	1.72147789149953
N	-2.39109600732338	-1.51296614862789	1.72147786183068
N	2.50666009931615	-1.31573295314470	1.72147789806482
C	0.07224699228415	-1.80108698543770	-1.14619002345440
C	-0.13041505107113	-4.11164795495645	-2.18211904755730
C	0.82403795398689	-4.70774498223375	-3.02209305697694
C	0.58144305068950	-6.01761402866421	-3.43271992949044
H	1.20643398389191	-6.45539199179053	-3.99806502522382
C	-0.55997699609748	-6.68780700241233	-3.02443199805857
H	-0.70708801693718	-7.58148698880073	-3.31368502762737
C	-1.48980894385988	-6.07251904200057	-2.20083688533869
H	-2.26822102070346	-6.54867798304272	-1.93615104180884
C	-1.30099603182427	-4.76411698209849	-1.75569806362111
C	1.52443198991737	0.96177802095443	-1.14618999775067
C	3.62676798477720	1.94154791825266	-2.18211906290267
C	3.66577700848229	3.06617695225309	-3.02209305726949
C	4.92145399758139	3.51101806864495	-3.43271991853023
H	4.98808499858690	4.27116597479560	-3.99806503034153
C	6.07256799946769	2.85761600416831	-3.02443199807661
H	6.92007300007017	3.17705397555186	-3.31368502917625
C	6.00462901235177	1.74471406959757	-2.20083688509740
H	6.80619999426772	1.30866897281720	-1.93615104143639
C	4.77711200046033	1.25402995893609	-1.75569806521639
C	-1.59437200029684	0.83797399928600	-1.14619001082193
C	-3.49404496911689	2.16876600948027	-2.18211902940647
C	-4.48750697971166	1.64023401917870	-3.02209302264397
C	-5.50058905909742	2.50526196405659	-3.43271991995266
H	-6.19221197237674	2.18289201416789	-3.99806503867770
C	-5.51028400269728	3.82885700235101	-3.02443199205556
H	-6.21067799404097	4.40309900342493	-3.31368501051936
C	-4.51251300143748	4.32647100253750	-2.20083700398327
H	-4.53567200127714	5.23867499599896	-1.93615099338085
C	-3.47380997051199	3.50875301641639	-1.75569804140917
C	-0.07063202445617	1.80015300652322	1.14414299538942
C	0.13203005802668	4.11071394778363	2.18007105406925
C	-0.82242295931410	4.70681198079966	3.02004505417666
C	-0.57982805145876	6.01668003192015	3.43067293192696
H	-1.20412698187760	6.45405898847757	3.99514002613121
C	0.56159199704642	6.68687399975518	3.02238499699704
H	0.70939601838067	7.58015398588470	3.31076003295139
C	1.49142394523829	6.07158604425466	2.19878888515762
H	2.27052902193393	6.54734498030067	1.93322704153007
C	1.30261103298164	4.76318298420806	1.75365006322854
C	-1.52281699103276	-0.96271198778381	1.14414303002391

C	-3.62515298277202	-1.94248192398838	2.18007105507217
C	-3.66416200713885	-3.06711094577171	3.02004506153183
C	-4.91983899612917	-3.51195207307371	3.43067292217183
H	-4.98577699758078	-4.27249897723374	3.99514003004617
C	-6.07095299822686	-2.85855000191760	3.02238499781447
H	-6.91776599910706	-3.17838797784643	3.31076003463724
C	-6.00301401127248	-1.74564807390022	2.19878888251275
H	-6.80389299326913	-1.31000197013126	1.93322704128592
C	-4.77549699958467	-1.25496396057147	1.75365006676401
C	1.59598701195895	-0.83890797873534	1.14414299589452
C	3.49565993385343	-2.16970002151494	2.18007104793778
C	4.48912196164734	-1.64116802934392	3.02004505594706
C	5.50220405149374	-2.50619596872379	3.43067293125237
H	6.19451998171045	-2.18422600780281	3.99514002582758
C	5.51189900299387	-3.82979099755516	3.02238499801490
H	6.21298497738917	-4.40443201238454	3.31076003328361
C	4.51412806552453	-4.32740497284839	2.19878888133105
H	4.53797997275931	-5.24000901059741	1.93322704283644
C	3.47542496699628	-3.50968602211978	1.75365006614130
H	-2.69142517662955	3.88661904318476	-1.11422216522473
H	-4.44666781173988	0.59474277858598	-3.31466207619015
H	-1.70764960859551	4.14935408555847	3.31325305598250
H	2.00050565294985	4.24880212933919	1.09846864147604
H	-4.67919003729045	-0.39327240645814	1.09862119779561
H	-2.73853097876341	-3.55535932718100	3.31200047799349
H	2.68126553109952	-3.85708545308039	1.09831925709349
H	4.44875661681843	-0.59568111974605	3.31283944558041
H	2.74014633859801	3.55430461790790	-3.31425589670369
H	4.68074795462181	0.39220857651452	-1.10084677750461
H	-1.99889393115994	-4.24975037723547	-1.10050409529969
H	1.70921945881877	-4.15025748909152	-3.31539175616540

## References

- (1) Manzer, L. E. Tetrahydrofuran Complexes of Selected Early Transition Metals. *Inorg. Synth.* **1982**, *21*, 135–140.
- (2) Sattler, W.; Ener, M. E.; Blakemore, J. D.; Rachford, A. A.; Labeaume, P. J.; Thackeray, J. W.; Cameron, J. F.; Winkler, J. R.; Gray, H. B. Generation of Powerful Tungsten Reductants by Visible Light Excitation. *J. Am. Chem. Soc.* **2013**, *135*, 10614–10617.
- (3) Barybin, M. V.; Young, V. G.; Ellis, J. E. First Paramagnetic Zerovalent Transition Metal Isocyanides. Syntheses, Structural Characterizations, and Magnetic Properties of Novel Low-Valent Isocyanide Complexes of Vanadium. *J. Am. Chem. Soc.* **2000**, *122*, 4678–4691.
- (4) Sheldrick, G. M. SADABS, Version 2.03, Bruker Analytical X-Ray Systems, Inc., Madison, WI. 2000.
- (5) SAINT and APEX 2 Software for CCD Diffractometers, Bruker AXS Inc., Madison, WI. 2014.
- (6) Sheldrick, G. M. A Short History of SHELX. *Acta Crystallogr. A* **2008**, *64*, 112–122.
- (7) Daul, C.; Schläpfer, C. W.; Mohos, B.; Ammeter, J.; Gamp, E. Simulation of EPR-Spectra of Randomly Oriented Samples. *Comput. Phys. Commun.* **1981**, *21*, 385–395.
- (8) Abragam, A.; Bleaney, B. *Electron Paramagnetic Resonance of Transition Ions*; Clarendon press, Oxford, 1970.
- (9) Rieger, P. H. Electron Paramagnetic Resonance Studies of Low-Spin  $d^5$  Transition Metal Complexes. *Coord. Chem. Rev.* **1994**, *135/136*, 203–286.
- (10) McGarvey, B. R. In *Transition Metal Chemistry*; Carlin, R. L., Ed.; Marcel Dekker: New York, 1966; p 90.
- (11) Stoll, S.; Schweiger, A. EasySpin, a Comprehensive Software Package for Spectral Simulation and Analysis in EPR. *J. Magn. Reson.* **2006**, *178*, 42–55.
- (12) Wapler, M. C.; Leupold, J.; Dragonu, I.; Von Elverfeld, D.; Zaitsev, M.; Wallrabe, U. Magnetic Properties of Materials for MR Engineering, Micro-MR and Beyond. *J. Magn. Reson.* **2014**, *242*, 233–242.
- (13) Bain, G. A.; Berry, J. F. Diamagnetic Corrections and Pascal's Constants. *J. Chem. Educ.* **2008**, *85*, 532–536.
- (14) de Levie, R. SolverAid. 2012.
- (15) Chakarawet, K.; Davis-Gilbert, Z. W.; Harstad, S. R.; Young, V. G.; Long, J. R.; Ellis, J. E. Ta(CNDipp)<sub>6</sub>: An Isocyanide Analogue of Hexacarbonyltantalum(0). *Angew. Chem., Int. Ed.* **2017**, *56*, 10577–10581.



- (16) Bersuker, I. B.; Blake, A. B. The Jahn–Teller Effect and Vibronic Interactions in Modern Chemistry. *Anal. Chim. Acta* **1987**, *201*, 371.
- (17) Englman, R. *The Jahn-Teller Effect in Molecules and Crystals*; John Wiley & Sons, Ltd: London, 1972.
- (18) Atanasov, M.; Comba, P.; Daul, C. A.; Hauser, A. DFT-Based Studies on the Jahn–Teller Effect in 3d Hexacyanometalates with Orbitally Degenerate Ground States. *J. Phys. Chem. A* **2007**, *111*, 9145–9163.
- (19) Bunting, P. C.; Atanasov, M.; Damgaard-Møller, E.; Perfetti, M.; Crassee, I.; Orlita, M.; Overgaard, J.; van Slageren, J.; Neese, F.; Long, J. R. A Linear Cobalt(II) Complex with Maximal Orbital Angular Momentum from a Non-Aufbau Ground State. *Science* **2018**, *362*, eaat7319.